Investigating Tom1 as a Candidate Regulator of Ptch1

by

Michelle A. Crawford

Submitted in partial fulfilment of the requirements
for the degree of Master of Science

at

Dalhousie University
Halifax, Nova Scotia
December 2012

DALHOUSIE UNIVERSITY

DEPARTMENT OF ANATOMY AND NEUROBIOLOGY

The undersigned hereby certify that they have read and recommend to the Faculty of Graduate Studies for acceptance a thesis entitled "Investigating Tom1 as a Candidate Regulator of Ptch1" by Michelle A. Crawford in partial fulfilment of the requirements for the degree of Master of Science.

Dated: December 3rd, 2012

Supervisor: _____

Readers: _____

_____

_____

DALHOUSIE UNIVERSITY

DATE: December 3rd, 2012

AUTHOR: Michelle A. Crawford

TITLE: Investigating Tom1 as a Candidate Regulator of Ptch1

DEPARTMENT OR SCHOOL: Department of Anatomy and Neurobiology

DEGREE: MSc CONVOCATION: May YEAR: 2013

_____

Signature of Author

TABLE OF CONTENTS

LIST OF TABLES

LIST OF FIGURES

ABSTRACT

Sonic hedgehog (Shh) is a signaling molecule that is involved in patterning the embryo and regulates adult stem cell homeostasis. Patched1 (Ptch1) is the receptor for Shh and upon binding to Shh is endocytosed, allowing downstream signaling to occur. Ptch1 is critical to the cellular response to Shh because it is both a negative regulator of the Shh signaling pathway and a transcriptional target of the pathway. Therefore, the regulation of Ptch1 levels will directly affect the ability of cells to respond to Shh. Understanding this process requires the characterization of novel Ptch1-interacting proteins that regulate Ptch1 levels in the cell. This thesis investigated a role for the adapter protein Tom1 as a putative Ptch1-interacting protein involved in regulating Ptch1 levels through endocytic cycling. It was found that Tom1 overexpression did not regulate the patterning of vertebrate nervous system, but did play a role the sub-cellular localization of Ptch1.

LIST OF ABBREVIATIONS AND SYMBOLS USED

AF1	activating factor 1
bp	base pair
C-terminal	carboxyl terminal
cDNA	complimentary deoxyribonucleic acid
CFTR	cystic fibrosis transmembrane conductance receptor
CGNP	cerebellar granular neuronal precursor
Ci	cubitus interruptus
CNS	central nervous system
DAB	3,3'-Diaminobenzidine
DdEps15	*Dictyostelium discoideum* epidermal growth factor receptor substrate 15
DdTom1	*Dictyostelium discoideum* target of myb 1
DdTsg101	*Dictyostelium discoideum* tumor susceptibility gene 101
DEPC	diethylpyrocarbonate
DK	donkey
DMEM	Dulbecco's modified Eagle's medium
DNA	deoxyribonucleic acid
E	embryonic
ECL	electrogenerated chemiluminescence
EDTA	ethylenediaminetetraacetic acid
EGF	epidermal growth factor
EGFP	enhanced green fluorescent protein
EGFR	epidermal growth factor receptor
ENU	*N*-ethyl-*N*-nitrosourea
ESCRT	endosomal sorting complex required for transport
FGF8	fibroblast growth factor 8
fp/FP	floorplate
Gas1	growth arrest-specific protein 1
GAT	GGA and Tom1
GCL	granular cell layer
Gli	glioma associated oncogene homolog
HEK293	human embryonic kidney cell line 293
HH	Hamburger and Hamilton stage
Hh	ghedgehog
HI-FBS	heat inactivated fetal bovine serum
HRP	horseradish peroxidase
Hrs	hepatocyte growth factor regulated tyrosine kinase substrate
IgG	immunoglobulin G
IL-1R	interleukin 1 receptor
IL-1β	interleukin 1 beta
IP	immunoprecipitate
ISH	*in situ* hybridization
LB	

LBPA	lysobisphosphatidic acid
LC3	microtubule-associated protein 1 light chain 3
LPS	lipopolysaccharide
MCL	molecular cell layer
miRNA	micro ribonucleic acid
mRNA	messenger ribonucleic acid
Ms	mouse
MVB	multivesicular body
N-terminal	amino terminal
NBT	nitro blue tetrazolium chloride
NCBI	National Centre for Biotechnology Information
NEB	New England Biolabs
Nedd4	neural precursor cell expressed developmentally down-regulated protein 4
NF-Kβ	nuclear factor kappa-light-chain enhancer of activated B cells
NPC1	Niemann-Pick Disease type C1
OCT	optimal cutting temperature
Olig2	oligodendrocyte transcription factor 2
Pax6	paired box 6
Pax7	paired box 7
PBS	phosphate buffered saline
PBT	phosphate buffered saline 0.1% Triton-X-100
PCL	Purkinje cell layer
PCR	polymerase chain reaction
PEI	polyethylenimine
PFA	paraformaldehyde
pMN	motoneuron progenitor
Ptch1	patched1
$Ptch1^{Wig}$	patched1 Wiggable mutant
PVDF	Polyvinylidene fluoride
RE	restriction endonuclease
RT	room temperature
RT-PCR	reverse transcription polymerase chain reaction
SARA	smad anchor for receptor activation
Shh-N	Sonic hedgehog N-terminus
siRNA	short interfering RNA
Smo	smoothend
SSC	saline-sodium citrate
SSD	sterol sensing domain
STAM	signal transducing adapter molecule
TBS	tris buffered saline
TBST	tris buffered saline 0.1% Tween-20
TGFβ	transforming growth factor β
Tollip	toll interacting protein
Tom1	target of Myb1
Tom1L1	Tom1-like protein 1

Tom1L2	Tom1-like protein 2
VHS	Vps27, Hrs and STAM
Vps27	vacuolar protein sorting 27

ACKNOWLEDGEMENTS

I wish to first and foremost thank my supervisor, Dr. Angelo Iulianella for the immense amount of time and effort he put into training me throughout my entire degree. Second I would like to thank my committee for their help and guidance. Finally, I would like to thank my colleagues, friends, and family for their support while completing my studies.

CHAPTER 1: INTRODUCTION

A central question in developmental biology is how various cell types arise and become organized in precise spatial arrangements, such as those found in the central nervous system (CNS). The formation of distinct cell types during embryogenesis is highly dependent upon the precise spatio-temporal control of evolutionarily conserved signaling molecules. These include those from the transforming growth factor ß (TGF-ß) superfamily, the Wnt family and the hedgehog (Hh) family. Furthermore, these signaling molecules continue to be expressed in the adult, and can have diverse effects on their target cells depending on the context of the receiving cell. We are now starting to understand some of the molecular mechanisms that direct these diverse effects within cells, but uncovering novel regulators will be important for ultimately understanding how cells receive and interpret these extracellular signals.

The Sonic Hedgehog Signaling Molecule

Shh is a Regulator of Developmental Patterning

In *Drosophila* there is only one Hh protein, while in vertebrates there are three members of the Hh signaling family; Sonic hedgehog (Shh), Indian hedgehog and desert hedgehog. However, Shh is the best studied, and is the main Hh signaling protein in the nervous system. Shh is involved in the development of many organs and systems including the gut, pancreas, and the CNS. It also plays a vital role in the patterning of the CNS, the limb skeletal elements and digit identity. Furthermore, Shh has been shown to regulate cell proliferation and axon guidance and is involved in maintenance of adult

stem cells (Rowitch et al., 1999; Kenny et al., 2003). Shh acts as a proliferation-inducing agent, and as a result activating mutations in the Shh pathway can cause cancer. Indeed aberrant Shh signaling is observed in approximately 20% of cancers (Kar et al., 2012).

The receptor for Shh is called Patched1 (Ptch1), and it acts as a negative regulator of the pathway. In this way, it also acts as a tumor suppressor in cancers that are caused by excess Shh signaling. Furthermore, inactivating mutations in the Ptch1 gene are well known to cause cancer. Two of the most notable cancers caused by mutations in Ptch1 are basal cell carcinoma, the most common form of skin cancer in the Western world, and medulloblastoma, a malignant cancer that affects the developing cerebellum (Lindstrom et al., 2006; Slade et al., 2010). Indeed the targeting of Ptch1 by therapeutics is an active area of research into the treatment of cancer (Nakamura et al., 2012). Identifying novel regulators of Ptch1 will enable us to better understand and manipulate Shh signaling in the case of disease.

Shh is considered to be a morphogen. Famously described by Louis Wolpert, a morphogen is "a signaling molecule that acts directly on cells to produce specific cellular responses dependent on its concentration" (Wolpert, 1969). Therefore, the concentration of the morphogen is thought to provide positional identity to its receiving cells. In the case of Shh patterning the ventral nervous system, cells that are closest to the source receive highest concentrations of Shh and develop into one cell type. Similarly those that are further away from the signal receive lower amounts of Shh and develop into a different cell type (Figure 1). This pattern of cellular differentiation leads to the development of several distinct cell types based on the perceived level of Shh signaling

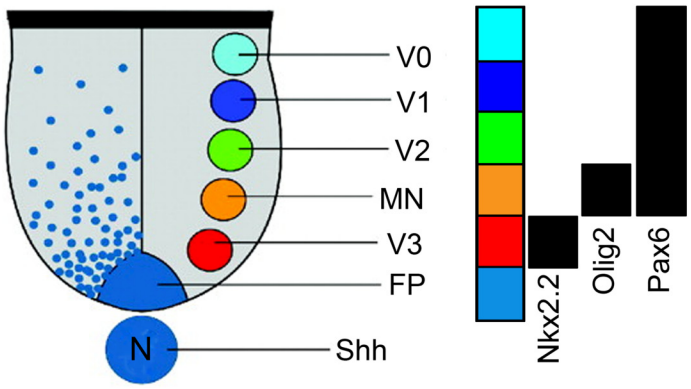

FIGURE 1. Progenitor domains induced by Sonic hedgehog (Shh) in the ventral neural tube. *Left,* Shh released from the notochord diffuses through the ventral neural tube and patterns ventral progenitor domains in a concentration dependent manor. *Right,* Schematic of transcription factor expression in progenitor domains. Nkx2.2 marks the V3 progenitor domain, while Olig2 specifically marks the MN progenitor domain. Pax6 marks all ventral progenitor domains except for the V3 and flooorplate progenitors. Floorplate (FP). V3 interneuron progenitors (V3), Motoneuron progenitors (MN), V2 interneuron progenitors (V2), V1 interneuron progenitors (V1), V0 interneuron progenitors (V0), notochord (N). Adapted from " Regulatory pathways linking progenitor patterning, cell fates and neurogenesis in the ventral neural tube" by J. Briscoe and B. Novitch, 2008, *Phil. Trans. R. Soc. B., 363,* p. 58.

However, this model is too simplistic and does not take into account several key problems. Shh is highly conserved from flies to humans where there is a large difference in size and cell number between embryos. Remarkably, patterning of tissues is maintained despite these differences. Furthermore, Hh binding proteins, including Ptch1, are largely responsible for shaping the extracellular Hh gradient (Ribes and Briscoe, 2009; Beachy et al., 2010). Adding further complexity, in addition to Shh concentration, the amount of time cells are exposed to Shh is critical for proper patterning of the vertebrate nervous system (Jeong and McMahon, 2005; Dessaud et al., 2007). These findings all suggest that receiving cells are not passive recipients of the Shh signal, but instead play an active role in establishing and interpreting the Shh gradient.

Shh Patterns Ventral Progenitor Domains in the Vertebrate Neural Tube

Vertebrate Shh signaling has been most intensely studied in the developing nervous system. Shh released from the notochord (a rod of embryonic mesoderm underlying the neural tube) patterns the ventral half of the neural tube in a concentration dependent manner (Ecricson et al., 1997; Briscoe et al., 1999; Matise and Wang, 2011). Shh diffusing from the notochord induces the floorplate (fp) which then also begins to release Shh. Floorplate released Shh induces the establishment of ventral progenitor domains. These are distinct domains of progenitor cells each characterized by the expression of a specific combination of homeodomain transcription factors. From ventral to dorsal the progenitor domains are: V3 interneurons, motoneurons, V2 interneurons, V1 interneurons (Figure 1). Each of these domains can be visualized using antibodies against domain specific transcription factors (Figure 1). Given the well-defined progenitor domains that

develop in response to graded Shh signaling the developing neural tube is an ideal system to study Shh signaling dynamics.

Shh in the Cerebellum

In addition to effects on patterning, Shh has a well-known role in regulating proliferation. This is best exemplified by Shh induced cerebellar granular neuronal precursor (CGNP) proliferation in the developing cerebellum. Shh diffusing from Purkinje cells causes the expansion of the CGNP pool in the rostral rhombic lip (Vaillant and Monard, 2009). These expanded precursors then migrate to the external granular layer where they further proliferate in response to Shh signaling. The CGNPs continue to migrate past the molecular layer and Purkinje cells to their final location, which is the internal granular cell layer (Vaillant and Monard, 2009). Shh is thought to induce proliferation primarily by upregulating the expression of the protooncogene n-Myc (Kenney et al., 2003).

Purkinje cells continue to express Shh in the adult cerebellum as well as downstream components of Shh signaling, including Ptch1 and the co-receptor smoothend (Smo). Interestingly, in the adult rat cerebellum Ptch1 and Smo localize to the dendritic spines, endosomes, and autophagosomes (Petrolia et al, 2012). While the significance of this localization in unknown, it suggests that the subcellular localization of the Shh pathway components is important for the biology of certain cell types in the adult brain. However, it is unknown how cells receive and interpret Shh differently during development and the adult such that overproliferation and cancer do not occur.

Modification of the Shh Protein

Full length Shh protein is a 45kD protein. The carboxyl terminus (C-terminus) catalyzes the cleavage of Shh creating a biologically active 22kD amino terminal (N-terminus) domain and a 25kD C-terminal domain with no known role in signaling. Concurrent with cleavage, a cholesterol moiety is added to the C-terminus of the N-terminal domain, while the N-terminus is S-palmitoylated by the enzyme hedgehog acyltransferase (Porter et al., 1996; Lewis et al., 2001; Buglino and Resh, 2008; Dennis et al., 2012). These modifications are important for the secretion, spread and activity of Shh. In particular, cholesterol is important in determining the Shh extracellular gradient size and shape (Caspary et al., 2002; Ma et al., 2002; Tian et al, 2004). Secretion of modified Shh from the cell requires Dispatched-1, a transmembrane protein that is functionally related to Ptch1. Furthermore Ptch1 has an active role in removing cholesterol modified Shh from Shh producing cells (Etheridge et al., 2010).

Downstream Shh Signaling Cascade

Shh binds to its receptor Ptch1. Ptch1 is a twelve pass transmembrane receptor, found at the cell surface. Ptch1 is thought to have a dual role in Shh signaling. It functions to transduce Shh intracellularly, but Ptch1 also sequesters Shh and prevents excess spread through the extracellular matrix (Torroja et al., 2004; Matise and Wang, 2011). Unbound Ptch1 acts as a negative regulator of the Shh signaling pathway by inhibiting the G-protein related transmembrane protein Smo (Rohatghi et al., 2007). Smo is the effector of the Shh signaling pathway, and upon binding of Shh

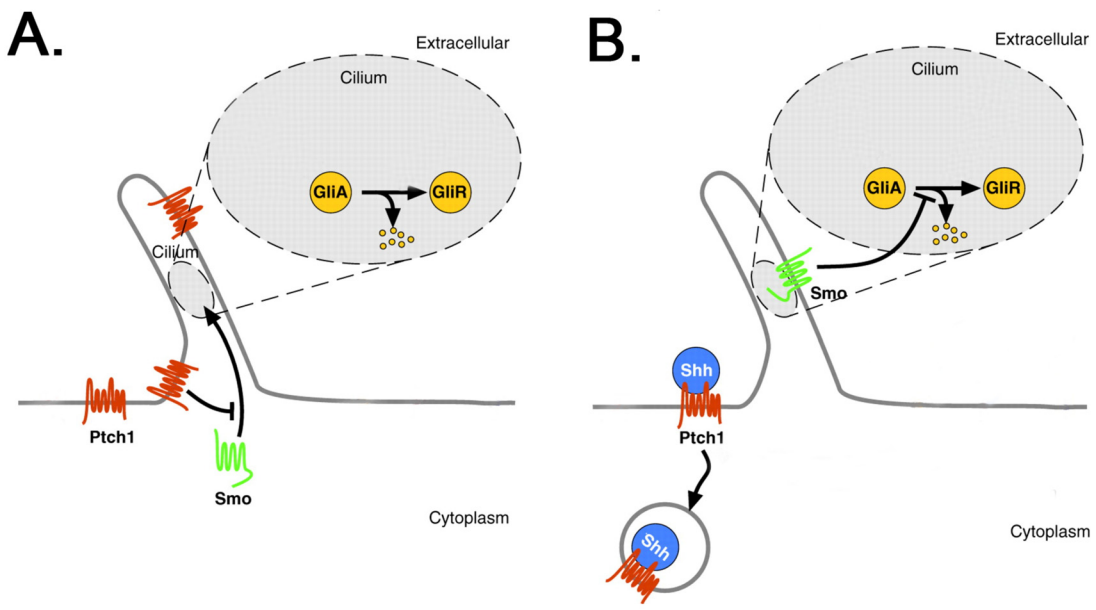

FIGURE 2. Shh signaling in vertebrate cells. (A) In the absence of Shh, Ptch1 inhibits the localization of Smo to the primary cilium through a poorly defined mechanism. The absence of Smo at the cilium causes Gli activator (GliA) to be proteolytically cleaved into its repressor form (GliR). (B) Shh binding to Ptch1 causes the removal of Ptch1 from the base of the primary cilium allowing Smo translocate there and prevent the cleavage of GliA allowing it to activate Shh responsive genes, including Ptch1. Adapted from "Pattern formation in the vertebrate neural tube: a sonic hedgehog morphogen-regulated transcriptional network" by E. Dessaud, A. McMahon, and J. Briscoe, 2008, *Development, 145*, p. 2490.

to Ptch1, Smo is derepressed and translocates to the cell surface allowing it to activate downstream target genes (Figure 2; Zhu et al., 2003; Wang et al., 2009). When activated, Smo prevents the processing of glioma associated oncogenes (Gli) zinc finger transcription factors into their repressor forms (Figure 2). In *Drosophila*, Smo only regulates the zinc finger transcription factor cubitus interruptus (Ci), but in vertebrates there are three homologues to Ci; Gli1, Gli2 and Gli3. Gli1 and Gli2 are primarily responsible for the activation of Shh target genes, while Gli3 primarily acts as a repressor of Shh signaling (Stamataki, 2005). Shh target genes include the transcription factors Olig2, Nkx2.2, Pax6 and Ptch1 (Figure 1). Since Ptch1 is both a negative regulator and a target of Shh signaling it plays an important role in interpreting the cellular response to Shh.

The Patched1 Receptor in Shh Regulation

Ptch1 Controls Shh Signaling

The Ptch1 protein is highly conserved from *Drosophila* to humans. It is characterized by two large extracellular loops, a sterol sensing domain (SSD) and a C-terminal intracellular domain (Figure 3; Jenkins et al., 2009). The two large extracellular loops are responsible for binding Shh, while the C-terminus mediates the turnover of Ptch1 (Brisco et al., 2001; Lu et al., 2006). The C-terminus is also predicted to mediate the formation of Ptch1 homotrimers and has a PPXY motif that binds to the E3 ubiquitin ligases Smurf2 and Nedd4 (Lu et al., 2006; Kawamura et al., 2008).

The SSD is composed of the intracellular domains of transmembrane domains 2-6. Mutations in the SSD abolish Ptch1 inhibition of Smo and cause Ptch1 to accumulate

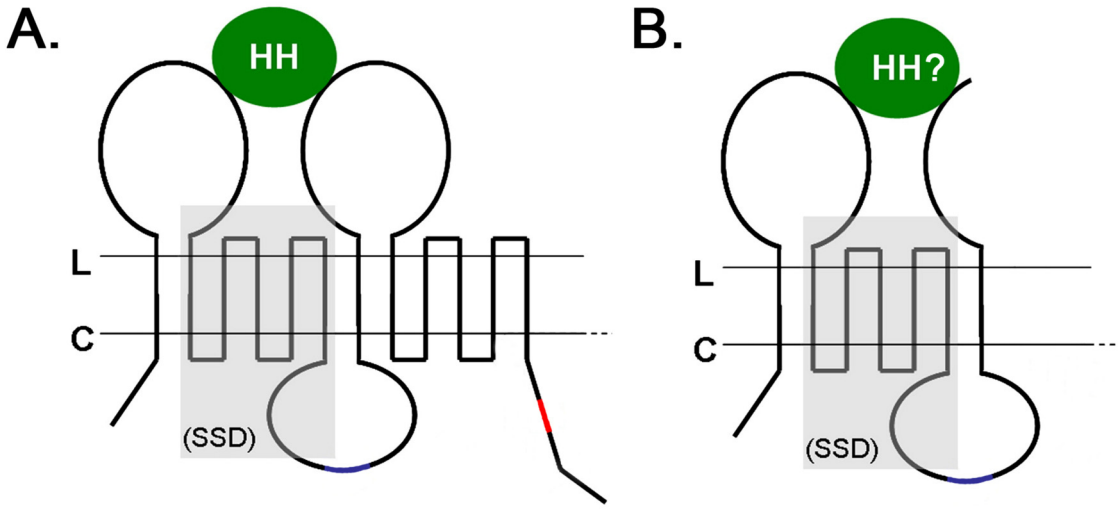

FIGURE 3. Schematic diagram of wild-type Ptch1 and Ptch1^{Wig} protein domains. (A) Wild-type Ptch1 showing 12 transmembrane domains, two large extracellular loops, a sterol sensing domain (SSD), and a C-terminal domain. The two extracellular loops bind Hh, and the C-terminal domain is important for Ptch1 turnover. The SSD forms from transmembrane domains 2-6 and is thought to be important for transporting a small molecule across the membrane and may be important for endocytic cycling. (B) The Patched1^{Wiggable} (Ptch1^{Wig}) mutant is prematurely truncated after the 7th transmembrane domain. Therefore it is missing the C-terminal domain that regulates its turnover. It is unknown if it is still able to bind Hh but does have an intact SSD. Adapted from " Hedgehog signaling: Emerging evidence for non-canonical pathways" by D. Jenkins, 2009, *Cellular Signaling, 21*, p. 1028.

in endosomal structures. This suggests it may mediate endocytic sorting of Ptch1 (Strutt et al., 2001; Martin et al., 2001). Interestingly, this region bears sequence similarity to the sterol-sensing domain in the Neimann-Pick Disease Type C1 (NPC1) protein. Originally identified by mutations that cause Neimann-Pick Disease Type C this protein is involved in intracellular cholesterol trafficking (Scott and Ioannou, 2004). Like Ptch1, NPC1 forms homotrimers and when co-expressed both proteins co-localize extensively in late endosomes (Incardona et al., 2000a). Ptch1 also seems to be involved in cholesterol transport and causes cholesterol efflux from cells (Bidet et al., 2011).

The exact mechanism of how Ptch1 controls Smo activation is unknown. What is known is that Ptch1 inhibits Smo sub-stoichiometrically, which suggests that there is no physical interaction between Ptch1 and Smo (Taipale et al., 2002). Furthermore, the ratio of Shh bound to unbound Ptch1, rather than the absolute levels, is more important for controlling Smo activation (Casali and Struhl, 2004). Smo localization to the plasma membrane is critical for its function. In *Drosophila,* localization of Smo to the plasma membrane seems to be necessary and sufficient for pathway activation (Zhu et al., 2003). In vertebrates, Shh signaling takes place at the primary cilium, a single protrusion found on nearly every cell (Figure 2; Corbit et al., 2005; Rohatgi et al., 2007). Indeed Smo and other downstream components of Shh signaling localize to the primary cilium upon pathway activation (Rohatgi et al., 2007; Wilson et al., 2009). Ptch1 localizes to the base of the primary cilium until it is bound by Shh, causing its internalization and removal from the cell surface (Figure 2; Rohatgi et al., 2007).

Ptch1 is thought to prevent Smo localization to the primary cilium by controlling the flow of a small molecule across the plasma membrane. The identity of this molecule

is not known but Shh pathway can be activated by cholesterol derivatives including 20-αhydroxycholestrol (Stanton and Peng, 2009). Indeed, binding of Shh to Ptch1 inhibits cholesterol efflux and causes Smo accumulation at the plasma membrane; however, this is not sufficient for pathway activation in vertebrates (Bidet et al., 2011). Together this suggests controlling levels and subcellular localization of Ptch1 within the cell is important for Smo activation and therefore downstream Shh signaling.

The Patched1^{Wiggable} Mutant

Through an ENU (*N*-ethyl-*N*-nitrosourea) mutagenesis screen, our group identified a novel Ptch1 mutant named *Patched1^{Wiggable}* (*Ptch1^{Wig}*). *Ptch1^{Wig}* is the result of a single point mutation located in the 15th intron of *Ptch1* genomic DNA, causing an alternate splice acceptor site, a seven base pair insertion, and ultimately a premature truncation of the C-terminus after the 7th membrane-spanning domain (Figure 3). This partially interferes with the second large extracellular loop of Ptch1, which is involved in the binding of Shh, rendering it unknown whether Shh is able to bind to Ptch1^{Wig}. While *Ptch1* null mutants are lethal and embryos die at approximately E9.5 days in mice, *Ptch1^{Wig}* mutants live until E11.5 or E12.5. This suggests that Ptch1^{Wig} maintains some functionality through its N-terminus. Ptch1^{Wig} embryos are larger than wild-type embryos of the same stage, indicating this mutation results in overproliferation. In addition, they have highly disorganized craniofacial structures, vasculature, and ectopic ganglia (unpublished data). Of note, Ptch1^{Wig} does have an intact SSD, however it is unknown if it is functional. Given that the Ptch1 C-terminus mediates Ptch1 turnover,

Ptch1^{Wig} is expected to be more stable than wild-type Ptch1 (Lu et al., 2006, Kawamura et al., 2008).

The Role of Endocytosis in Shh Signaling

Receptor-mediated endocytosis is the process by which cells internalize ligand-receptor complexes. Cell surface receptors are commonly targeted for endocytosis by the addition of an ubiquitin moiety (Figure 4; Schwartz and Patrick, 2012). This causes the recruitment of endocytic machinery, the creation of a clathrin coated pit and the invagination and eventual scission from the plasma membrane by dynamin (Sigismund et al., 2012).

Once internalized the resulting endosome travels through the endocytic pathway. It first matures into a sorting or early endosome that can be marked by the protein Rab5 (Rink et al., 2005). From here cell surface receptors can be recycled back to the plasma membrane, often by the removal of the ubiquitin by deubiquitinating enzymes (DUB), or they can be targeted for degradation (Sigismund et al., 2012). Endosomes targeted for degradation mature into a late endosome or multivesicular body (MVB) marked by the protein Rab7 (Figure 4). Once the endosomes lose Rab5 and acquire Rab7 they are competent for fusion with the lysosome, which is filled with acid hydrolase enzymes that nonspecifically degrade the receptor-ligand complex (Figure 4; Rink et al., 2005).

From very early on it was noted that Hh accumulated in punctate structures throughout the cell (Tabata and Kornberg 1994; Capdevila et al., 1994). Later it was determined that binding of Hh to Ptch1 causes dynamin-mediated endocytosis of the

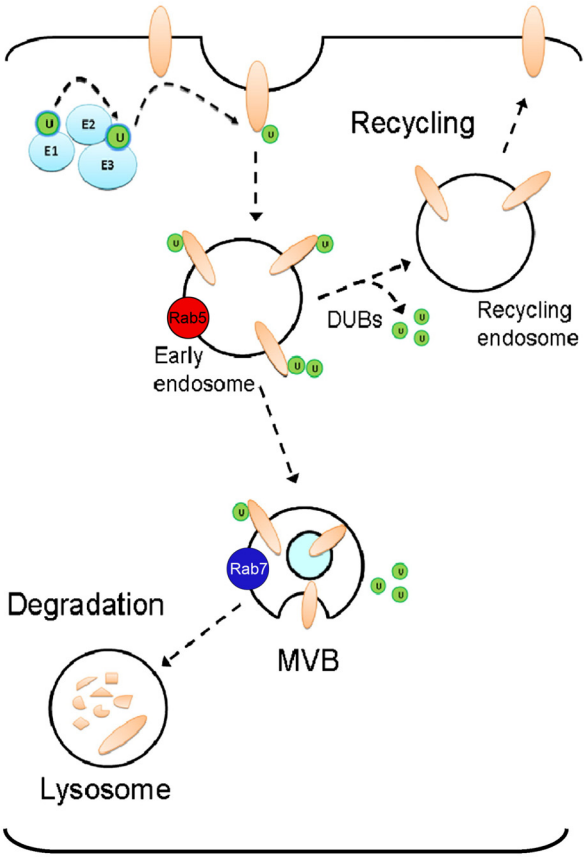

FIGURE 4. Endocytic cycling of cell surface receptors. Cell surface receptors are ubiquitinated by the action of ubiquitin activating, conjugating and ligating enzymes (E1, E2, E3 respectively) causing endocytosis. The resulting endosome matures into the early or sorting endosome, which can be marked by the protein Rab5. From here the ubiquitin moiety can be removed by deubquitinating enzymes (DUB) and receptors via the recycling endosome are returned to the cell surface. Alternatively, the early endosomal membrane invaginates and matures into a multivesicular body and is marked by the protein Rab7. The multivesicular body then fuses with the lysosome for degradation. Adapted from "Ubiquitin dependent endocytosis, trafficking and turnover of neuronal membrane proteins" by L. Schwartz and G. Patrick, 2012, *Molecular and Cellular Neuroscience,49,* p. 388.

complex in *Drosophila* as well as in vertebrates (Capdevila et al., 1994; Torroja et al., 2004, Incardona et al. 2000b). In contrast to most cell membrane receptors, when Ptch1 is overexpressed in cells, it is constitutively endocytosed with the majority of the protein localizing to late endosomes or lysosomes (Incardona et al., 2000; Gallet and Therond, 2005). In the presence of Smo, however, Ptch1 localizes more frequently to the cell surface and endocytosis is markedly reduced (Incardona et al., 2002; Gallet and Therond, 2004). Upon binding of Shh to Ptch1, both proteins are rapidly endocytosed and targeted to the lysosome for degradation in both vertebrate and invertebrate systems (Incardona et al., 2002).

Evidence suggests that endocytosis and endocytic cycling of Ptch1 is important for Hh signaling. Removal of Ptch1 from the plasma membrane by endocytosis is important for the concomitant increase in Smo localization to the plasma membrane (Denef et al., 2000). Torroja et al. (2004) found that blocking dynamin-mediated endocytosis of the Ptch1-Hh complex in the *Drosophila* wing imaginal disc inhibited the ability of Ptch1 to sequester Hh causing activation of target genes further away from the source than normal (Ingham and McMahon, 2001; Gallet and Therond, 2004). However inhibiting endocytosis or degradation of the Ptch1-Shh complex did not affect Shh target gene activation (Torroja et al., 2004). This suggests that the Hh signaling in *Drosophila* is conferred at the membrane and is not affected by endocytic cycling.

In contrast to Hh signaling in *Drosophila*, in vertebrates endocytic cycling seems to be required for proper Shh signaling. The lysobisphosphatidic acid (LBPA) antigen localizes to late endosomes, and incubation of cells with an anti-LBPA antibody disrupts late endosomal morphology and protein sorting. Incardona et al (2002) found that

incubating chick neural plate explants with anti-LBPA antibody impaired the ability of Shh to repress Pax7 gene transcription and induce Islet-1 and -2 transcription, which are targets of Shh signaling. This suggests that protein sorting in the late endosome has a pivotal role in Shh signaling. Despite these findings, our understanding of the regulators of Ptch1 and Shh endocytic cycling remains rudimentary.

Endocytic Regulation of Signaling and Target of Myb1

Endocytic Cycling and Signaling

It is estimated that over 30% of our genes are involved in the endocytic pathway, reflecting the importance of this process to cellular homeostasis (Wang et al., 2010). Previously thought to be quite simplistic, the endocytic pathway is proving to be important for many processes including cell signaling. Receptor mediated endocytosis was traditionally thought of as a means to attenuate signaling whereby removal from the cell surface ended signal transduction (Sigismund et al., 2012). However, mounting evidence indicates that endocytosed ligand and receptor can still be bound and actively signaling from within the cell (Wiley and Burke, 2001; Wang et al., 2004; Sigismund et al., 2008;). This suggests that the rate of endocytic cycling and degradation can have an effect on the duration of the signal and thus the cells interpretation of the strength of the signal. This has been demonstrated for several different signaling pathways including fibroblast growth factor 8 (Fgf8) and TGFβ (Julien and Gurdon, 2005; Nowak et al., 2011; Platta and Stenmark, 2011).

Interestingly, endocytic cycling not only affects the duration of signaling, but it can affect the activation of second messengers. Indeed blocking dynamin, a critical

component for endocytosis, allows the association of the TGFβ type I receptor with Smad anchor for receptor activation (SARA) and Smad2, but prevents the activation of Smad2/3, thus activating different downstream signaling pathways at the cell surface and on endosomes (Penheiter et al., 2002). In this way, functional versatility of cell surface receptors can be controlled by their dynamic subcellular localization.

In summary, the regulation of endocytic cycling can serve as a way for one signaling pathway to exert multiple effects on the cell. This may be the case for Shh signaling as its effects on the cell range from axon guidance, cell survival, proliferation, and differentiation. The tight control of endocytic cycling is likely required to ensure that the intended cellular effects in response to extracellular signaling occur in the right cell type and at the right time during development. Given the importance of Shh signaling to embryogenesis and cellular homeostasis, it is remarkable how little is understood regarding the regulation endocytic cycling of this pathway.

The Role of Ubiquitin in Signaling Protein Turnover and Function

The turnover and endocytic cycling of many cell surface receptors is regulated by ubiquitin (Piper and Lehner, 2011). Ubiquitin is 76 amino acid protein expressed in all eukaryotic cells. Its post-translational conjugation regulates the degradation and/or subcellular localization of a wide variety of proteins. Ubiquitin is attached to substrate proteins through the activity of three classes of enzymes: E1 ubiquitin activating enzymes, E2 ubiquitin conjugating enzymes and E3 ubiquitin ligases. Of these, E3 enzymes are the most numerous, allowing them to be highly specific to their target proteins (Figure 4; Hochstrausser, 1996).

Ubiquitin was first described by its ability to target proteins to the proteosome for degradation (Hochstrausser, 1996). However, mono-ubiquitination, or short chains of ubiquitin, have been shown to be involved in both altering the subcellular localization of proteins and targeting membrane proteins to the lysosome for degradation (Piper and Lehner, 2011).

Ubiquitination of transmembrane receptors targets them for endocytosis and the subsequent recruitment of the endosomal-sorting complex required for transport (ESCRT). There are four ESCRT complexes (ESCRT-0, I, II, III) that act in sequence to sort ubiquitinated membrane proteins into MVBs for degradation by the lysosome (Raiborg and Stenmark, 2009). The ubiquitinated transmembrane proteins are first recognized by hepatocyte growth factor regulated tyrosine kinase substrate (Hrs) and signal transducing adapter molecule (STAM), which together make up the ESCRT-0 complex (Raiborg and Stenmark, 2002). The ESCRT-0 complex binds ubiquitinated proteins and concentrates them into endosomal membrane subdomains and recruits the remaining ESCRT complexes I-III (Raiborg and Stenmark, 2009). ESCRT complexes I-III cause the formation of MVB by facilitating the invagination and pinching off of membrane proteins from the perimeter of the endosomal membrane (Raiborg and Stenmark, 2009). These proteins are important for regulating lysosomal degradation of cell surface receptors and when absent or dysregulated can affect downstream signaling pathways (Platta and Stenmark, 2011).

The Adapter Protein Target of Myb1

In a proteomic screen using human embryonic kidney (HEK293) cells stably transfected with Ptch1^{Wig}, our group identified Target of Myb1 (Tom1) as a putative interacting partner (unpublished findings). Tom1 is a 54kD protein that was originally discovered as a gene upregulated in response to the oncogene v-Myb (Burk et al., 1997). Since then, Tom1 has been established an adapter protein involved in endocytic trafficking and is thought to function in an alternative ESCRT-0 complex to Hrs and STAM (Wang et al., 2010). Adapter proteins are accessory proteins that do not have any inherent signaling ability, but instead mediate protein-protein interactions in signaling complexes (Flynn, 2001).

The Tom family of proteins consists of Tom1, Tom1L1 and Tom1L2. Tom1 and TomL2 are the most similar sharing 59% of amino acid sequences while Tom1L1 is more divergent, sharing only 30% and 31% sequence identity respectively (Wang et al., 2010). The homology between proteins is concentrated to the two protein domains that all three proteins share: the N terminal VHS (Vsp87, Hrs, STAM) domain and the central GAT (GGA and Tom) domain, while the C-terminus is comparatively divergent between the three proteins (Figure 5).

The VHS domain was originally identified by homology between vacuolar protein sorting 27 (Vsp87), Hrs, and STAM. It is 146 amino acids in length, consists of 8 alpha helices, and is always found at the N-terminus of the gene (Misra et al., 2000).

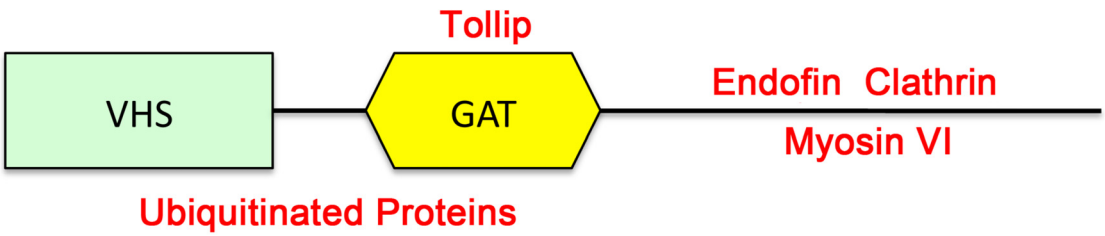

FIGURE 5. Structure and binding partners of Target of Myb1 (Tom1). Tom1 interacts with clathrin, endofin and myosin VI through its C-terminus while the GAT (GGA and Tom) domain mediates the interaction between Tom1 and Tollip. Tom1 binds ubiquitinated proteins by both the GAT and VHS domains (Vsp187, Hrs, STAM).

The GAT domain is found in only the GGA and Tom families of proteins, and mediates the interaction of Tom1 with ubiquitinated proteins and Toll interacting protein (Tollip; Figure 5; Shiba, 2003). Furthermore, Tom1 interacts with endofin (a FYVE containing protein that localizes to early endosomes), clathrin and myosin VI through its C-terminus (Figure 5). Primarily a cytosolic protein, Tom1 is targeted to the endosome by both Tollip and endofin (Yamanaki et al., 2003; Seet et al., 2004). Interestingly, Hrs also binds both clathrin and ubiquitinated proteins and is localized to the endosome (Raiborg and Stenmark, 2002). Given their similar binding partners, Tom1 is hypothesized to have a role mechanistically similar to Hrs acting as part of the ESCRT-0 complex, sorting ubiquitinated proteins into MVB (Wang et al., 2010). The importance of ESCRT-0 in Hh signaling was revealed by the knockdown of Hrs in *Drosophila*, which caused Ptch1 and Shh to accumulate in enlarged endosomes that stain positively for ubiquitinated proteins (Jékely and Rørth, 2003).

Unlike Hrs, which is evolutionarily conserved from yeast to humans, Tom1 is not present in yeast. However, a Tom1 homologue, termed DdTom1, is expressed in the amoeba *Dictyostelium discoideum*. Evidence of a role for Tom1 in the ESCRT-0 complex comes from a study with the amoeba *Dictyostelium discoideum* (Dd). DdTom1 has a conserved VHS and GAT domain, co-localizes with ubiquitinated proteins and binds to DdEps15 (EGFr pathway substrate), a protein involved in clathrin mediated endocytosis, and DdTsg101 (Tumor susceptibility gene 101), a component of the ancestral ESCRT-I complex (Blanc et al., 2009). Given this system did not have any other components of the ancestral ESCRT-0 complex, this provides evidence that Tom1 does function in a similar manor to Hrs.

The Role of Tom1 in Signaling

Tom1 has also previously been shown to have a functional role in the regulation of cell surface receptor endocytic cycling. Tom1 was found to co-immunoprecipitate with the interleukin 1 receptor (IL-1R; Brissoni et al., 2006). Upon binding, interleukin-1ß (IL-1ß) induces the ubiquitination of the IL-1R and this is thought to mediate the interaction with Tom1. Consistent with this, knocking out Tom1 impaired IL1-R endocytic cycling and degradation (Brissoni et al., 2006). The overexpression of Tom1 in cells stimulated by IL-1ß or tumor necrosis factor (TNFα) blunted the activation of the downstream transcription factors nuclear factor kappa-light-chain-enhancer of activated B cells (NF-KB) and activating factor 1 (AF1; Yamanaki and Yokosawa, 2004). Tollip is also known to play a similar role in IL1 signaling and is thought to link the IL-1R via Tom1 to the endosomal degradation machinery (Yamanaki and Yokosawa, 2004).

Interestingly, the microRNA miR-126 is a negative regulator of Tom1 protein levels and is downregulated in Cystic fibrosis airway epithelial cells (Ogelsby et al., 2010). Part of the disease process of Cystic fibrosis involves an aberrant upregulation of immune responses mediated by the Tom1 targets IL-1ß and TNFα. These findings underline the importance of Tom1 to normal cellular physiology and that its misregulation underlies the pathophysiology of at least one disease.

Autophagy

Autophagy is the process of the degradation of cytosolic components including damaged organelles and protein aggregates by the lysosome (Rubinsztein et al., 2012).

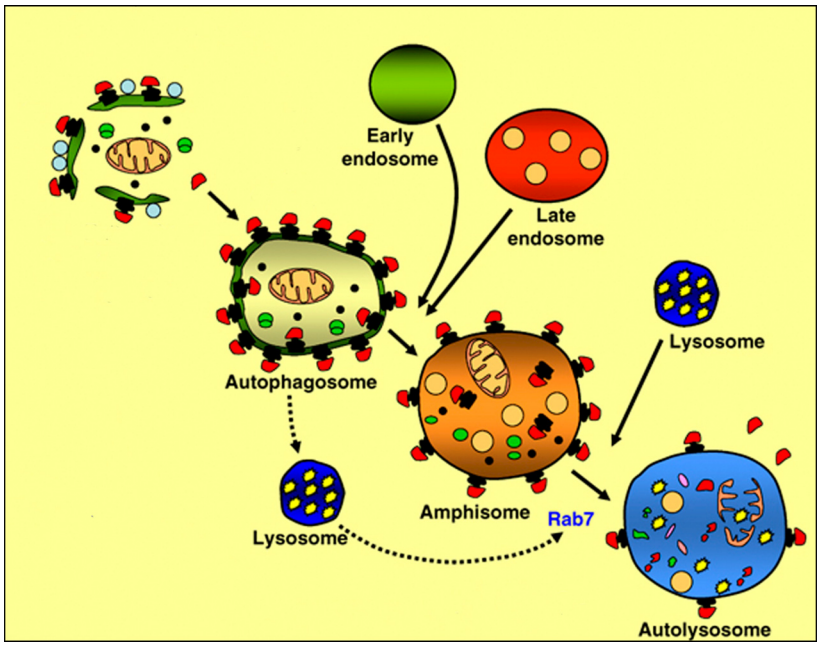

FIGURE 6. Convergence of the endocytic and autophagy pathways. Cytoplasmic material for degradation by autophagy is surrounded producing a double membrane structure called the autophagosome. The autophagosome can fuse directly with the lysosome for degradation, or fuses with early or late endocytic vesicles to produce the amphisome, which then also fuses with the lysosome for degradation. Adapted from "Autophagy and multivesicular bodies, two closely related partners" by C. M. Fader and M.I. Colombo, 2009, *Cell Death and Differentiation, 16,* p. 73.

Although there is a consistent basal level of autophagy occurring in cells, autophagy is highly activated under conditions of cell stress (Rubinsztein et al., 2012). Cell stress can occur from many stimuli such as amino acid starvation, or cell accumulation of mutant or mis-folded proteins. Cell contents targeted for autophagy are enclosed in a double membrane structure called an autophagosome (Rubinsztein et al., 2012). This structure then fuses with the lysosome resulting in the degradation of its contents (Figure 6: Rubinsztein et al., 2012).

During autophagosome formation microtubule associated light chain 3 (LC3) is cleaved, forming LC3II, and inserted into the autophagosome membrane. Consequently, the conversion of LC3I to LC3II is widely used as a measure for autophagosome activity as well as LC3 immunohistochemistry to visualize autophagosomes (Jin et al., 2012).

Autophagy is traditionally thought of as being the degradation route for large molecules such as damaged organelles; however it has been shown that MVB can also fuse with autophagosomes (Fader and Colombo, 2009). This fusion produces the amphisome, which then subsequently fuses with the lysosome for degradation (Figure 6). Interestingly, it was established that amphisome fusion with the lysosome was 5-6 times more likely than direct fusing of the autophagosome with the lysosome, suggesting that endosomal input to the autophagosome is not an uncommon phenomenon (Liou et al., 1997).

Autophagy has been brought into the spotlight recently because mutations in genes required for autophagy can cause the creation of protein aggregates observed in many diseases such as Alzheimer Disease, Parkinson Disease, and Cystic fibrosis (Rubinsztein et al., 2012). Furthermore, autophagy has also been shown to have a role in

cancer and aging. It is clear that proper regulation of autophagy is required for the maintenance of healthy cells (Rubinsztein et al., 2012).

Tom1 is Involved in Autophagy

Recently, components of the ESCRT complex have been shown to have an important role in autophagy (Rusten et al., 2008; Rusten and Stenmark, 2009). Indeed, knocking out components of the ESCRT machinery can cause the accumulation of LC3 positive autophagosomes (Filimonenko et al., 2007). In addition to the role of Tom1 in endosomal sorting, it was recently shown to target endosomes to the autophagosome (Tumberello et al, 2012). The retrograde actin protein myosin VI was found to bind Tom1 and that the deficiency of either protein resulted in the accumulation of LC3 positive autophagosomes (Tumberello et al, 2012). This is the same phenotype that occurs when knocking out components of the ESCRT complex, suggesting that Tom1 shares a similar role as the ESCRT complexes.

The Importance of Endocytic Cycling of Ptch1

Ptch1 is both a negative regulator and a transcriptional target of Shh. Furthermore, it also has a role in sequestering Shh, shaping the gradient of extracellular Shh. Therefore, controlling the levels and localization of Ptch1 is critical to gauging the cellular response to Shh signaling. Although it known that Ptch1 is endocytosed upon binding to Shh and is subsequently targeted to the lysosome for degradation (Incardona et al., 2000b, 2002), the regulation of this process is poorly understood. Given the diverse effects of Shh signaling and the mounting evidence that endocytic cycling is a critical regulator of how cells

receive and interpret extracellular signals, understanding the impact on Shh signaling is crucial. To unravel the specific effects of Shh signaling, we first need to identify regulators of this process. The **hypothesis** addressed in this thesis is that **Tom1 is an adapter molecule that regulates endosomal sorting and degradation of Ptch1,** and is predicted to alter the ability of cells to respond to Shh during neural development.

CHAPTER 2: MATERIALS AND METHODS

Animals:

Adult wild-type FVB mice were bred in the Carleton animal care facility of Dalhousie University and were maintained under a 12:12 light:dark cycle with the lights on at 7am. Food and water were available ad libitum. All animal procedures were conducted according to the guidelines of the Canadian Council on Animal Care and the Dalhousie University Animal Care Committee.

Mouse Embryo Preparation for In Situ Hybridization:

FVB mice were time mated and pregnant females were sacrificed at embryonic (E) stages E8.5, E9.5, and E10.5. Animals were paired overnight and checked for vaginal plugs in the morning. Noon of the day vaginal plug was found was designated stage E0.5. Embryos at E8.5-E10.5 were dissected from extra-embryonic tissues in ice cold diethylpyrocarbonate (DEPC) treated phosphate buffered saline (PBS) and fixed overnight in 4% paraformaldehyde (PFA; in DEPC-PBS) at 4°C. The following morning fixative was removed and embryos were rinsed in DEPC-PBS then dehydrated through a series of methanol dilutions (25%, 50% 75%/DEPC-PBS) to 100% methanol and stored at -20°C until ready for *in situ hybridization*.

Chick Embryo Preparation for In Situ Hybridization:

Fertilized eggs of *Gallus Gallus* were incubated at 38°C for 3.5 days (Hamburger and Hamilton (HH) stage 22). Embryos were dissected from extra-embryonic tissues, and fixed in 4% PFA (in DEPC-PBS) overnight at 4°C, dehydrated through a series of

methanol dilutions (25%, 50%, 75% in DEPC-PBS) to 100% methanol and stored at -20°C until ready for *in situ hybridization*.

Preparation of Embryos for Immunohistochemistry:

Mouse embryos at E9.5, E10.5 or chick embryos at E3.5 were dissected from extra embryonic tissues in PBS. Embryos were then fixed for 1 hour at RT in 4%PFA/PBS and then cryoprotected by equilibrating in 15% sucrose/PBS and 30% sucrose/PBS. Embryos were then embedded in Optimal Cutting Temperature (OCT, Tissue Tek) and stored at -80°C until sectioned. Embryos were sectioned on a cryostat at 12-14μm in transverse sections through the entire embryo.

Extraction of Total mRNA:

Total mRNA was extracted from E10.5 mouse and E3.5 chick embryos using the RNA*later*® kit (Invitrogen) according to the manufacturer's instructions. The quality and relative concentration of total mRNA was assessed by ethidium bromide-stained agarose gel electrophoresis.

Production of cDNA Library:

A complimentary DNA (cDNA) library of the tissue was generated from total mRNA extracted as described above using the Superscript® First-Strand Synthesis System for RT-PCR kit (Oligo dt primer; Invitrogen).

Cloning of Tom1 for Expression in Mammalian Cells:

The mouse target of myb1 (*mTom1)* cDNA sequence was obtained from National Centre for Biotechnology Information (NCBI) website (http://www.ncbi.nlm.nih.gov). To amplify *mTom1*, polymerase chain reaction (PCR) was conducted using the cDNA library. In order to facilitate cloning, mismatched primers surrounding the *mTom1* cDNA were used to create restriction endonuclease (RE) cut sites at the 3' (SacI) and 5'(EcoRI) ends of the gene (Table 1). DNA was digested with SacI and EcoRI (New England Biosciences; NEB) and ligated into the bicistronic eukaryotic expression vector pIRES2-EGFP (Clonetech) prepared with the same RE cut sites (Table 1). The resulting bicistronic vector produced both full length Tom1 and enhanced green fluorescent protein (EGFP; to monitor transfection efficiency) proteins.

A second mTom1 expressing plasmid, Tom1 pcDNA3.1, was constructed that does not expresses EGFP (Table 1). *Tom1* was isolated from *Tom1* pIRES2-EGFP using the XhoI and SalI RE and ligated into an empty pcDNA3.1 vector prepared with XhoI half sites. Empty pIRES2-EGFP, pEGFP-N1 (Clonetech), or pcDNA3.1 (Invitrogen) were used as negative controls to evaluate the specificity of Tom1 overexpression in cells and embryos.

Cloning of Tom1 for Riboprobe Synthesis:

To clone portions of the *Tom1* gene for riboprobe synthesis, primers were designed surrounding the cDNA coding region or 3' untranslated region of mouse or chicken *Tom1* cDNA (Burk, 0. *et al*. 1997; Table 2). Sequences were obtained from National Centre for Biotechnology Information (NCBI) website

Table 1. Mammalian expression plasmids of full length Tom1, Ptch1 and Ptch1^{Wig}.

Gene	Primer Sequence	Temp	Size (bp)	Accession number	Vector	Origin
mTom1	5'ctgcaggaattcagaccctacattc 3'tgattctggagctcgtggc	60°C	1500	NM_011622	pIRES2-EGFP	Constructed by Michelle Crawford
mTom1	Same as above	Same as above	1500	NM_011622	pcDNA3.1	Constructed by Michelle Crawford
mPtch1-Myc	NA	NA	4305	NM_008957.2	pRK5	Constructed by Dr.Iulianella
Flag-mPtch1^{Wig}	NA	NA	4305	NM_008957.2	pcDNA5/FRT	Constructed by Dr. Iulianella

(http://www.ncbi.nlm.nih.gov). In order to facilitate cloning, some primer pairs were designed with mismatched nucleotides to produce a RE cut site. Polymerase chain reaction (PCR) was then performed using the E10.5 mouse embryo, or E3.5 chick embryo cDNA library and gene specific primers outline in Table 2. The resulting PCR fragment was cut with REs (NEB) and directionally cloned into pBluescript (Thermo Scientific) or cloned directly following amplification via TA cloning into TOPO PCR 2.1 (Invitrogen).

Ligation, Transformation and Screening of Plasmid DNA

Ligations of plasmid DNA were conducted by incubating prepared insert and plasmid backbone (3:1) with T4 DNA ligase (NEB) at 14ºC overnight. Constructed plasmids were then subsequently transformed using chemically competent TOP10 cells (Invitrogen) and spread on lysogeny broth agar plates containing appropriate antibiotic. Colonies were screened by performing diagnostic digests using REs that release a fragment of a known molecular weight. Positive colonies were sent for sequencing at TCAG DNA Sequencing Facility (The Hospital for Sick Children Toronto, ON).

Riboprobe Synthesis:

Sense and anti-sense *Tom1* Plasmid DNA was linearized with appropriate RE and purified using phenol/chloroform (Table 2). RNA was transcribed from linear DNA using T7 or T3 RNA polymerase (NEB) and DIG RNA labeling mix (Roche). Positive control plasmids mouse Sonic hedgehog (*mShh)* and chicken Shh (*cShh*; kind gifts from Dr.

Table 2: Cloning of Tom1 for riboprobe synthesis.

Gene	Primer Sequence	Annealing Temp	Size	Accession number	Vector	RNA probe synthesis
mTom1 isoform 1	Fwd:acctgattctggagctggt Rev:gtatgagagtgtcaggccct	60°C	618 bp	NM_011622	Cloned into Blusescript (Clonetech) SacI and SmaI	SmaI/sense SacII/antisense
mTom1 isoform 1 3'UTR	Fwd:atggaggacattgagcagtg Rev:cagtggagggctgacttattc	58°C	401 bp	NM_011622	Bluescript (Clonetech)	SpeI/antisense
cTom1 3'UTR	Fwd:gccagtcgacatcagaagc Rev:ctttccaggctaacggca	63°C	445 bp	NM_205144	Bluescript (clonetech)	SalI/antisense XbaI/Sense

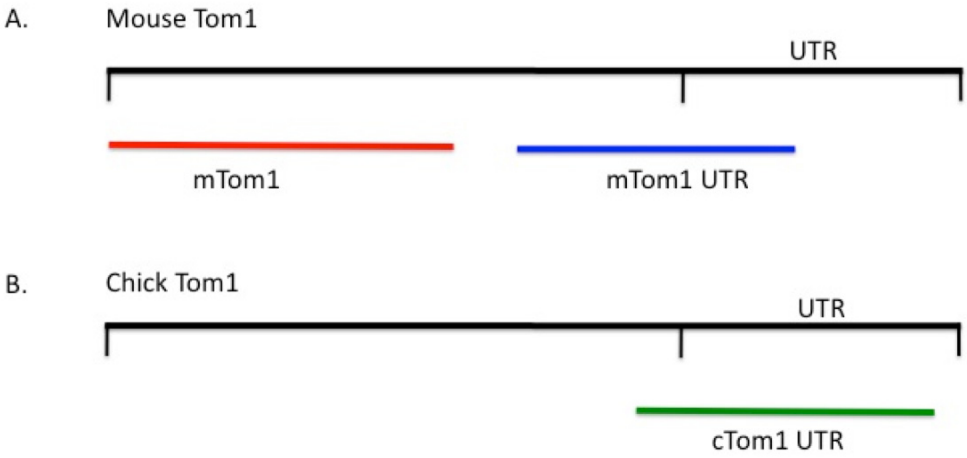

FIGURE 7. Tom1 riboprobe placement on mouse and chicken Tom1 cDNAs.

Andy McMahon) were linearized with HindIII and transcribed with T3 RNA polymerase. After transcription DNAse I (NEB) was added to digest the DNA template. RNA was precipitated using ammonium acetate and the relative concentration and size of RNA produced was assessed by ethidium bromide gel electrophoresis.

Whole Mount In Situ Hybridization:

Embryos stored in 100% MeOH were bleached for 2 hours in Dent's bleach (MeOH:H_2O_2:DMSO 4:1:1) and rehydrated to DEPC-PBT (Phosphate Buffered Saline + 0.1% Triton-X-100) through a series of methanol dilutions (75%, 50%, 25%/DEPC-PBT). Embryos were then treated with Proteinase K (10µg/mL NEB) for 5 min (mouse E9.5) or 10min (mouse E10.5 and chick E3.5) and rinsed immediately with glycine (2mg/mL)/PBT. Embryos were then post fixed in 4%PFA/0.25% glutaraldehyde for 20 minutes, rinsed and transferred to pre-warmed hybridization solution (50%formamide; 25%20XSSC; 0.01M EDTA ;0.1% Tween-20; 0.1% CHAPS; 50µg/mL heparin; yeast torula-RNA 1ug/mL; 20µg/mL Boehringer blocking powder) for 2 hours at 65°C. Riboprobe (approximately 1µg) was then added to embryos and incubated on a nutating platform at 65°C overnight. The next day the embryos were rinsed twice in post hybridization buffer (50% formamide; 25% 20X SSC; 0.1% Tween-20; 0.5% CHAPS), once in 50% post hybridization buffer (in 2X SSC/0.1% CHAPS), twice for 30 minutes in 2X SSC/0.1% CHAPS, and once for 30 minutes in 0.2XSSC 0.1% CHAPS. Embryos were then transferred to TBST (50mM Tris; 150mM NaCl; 0.1% Tween-20) for 30 minutes. Embryos were blocked in 20% heat inactivated goat serum for one hour at 4°C and DIG-alkaline phosphatase antibody (Roche) was added (1/2000) to serum and

incubated overnight at 4°C. The next day the embryos were washed throughout the day (changed once per hour) and overnight in TBST. To develop color, embryos were first equilibrated to alkaline phosphatase buffer (0.1M Tris/HCl pH9.5; 0.1M NaCl; 0.05M $MgCl_2$: 0.1% Tween-20) and then developed by adding NBT (340μg/mL) and BCIP (174μg/mL) (Roche) to embryos. Once the desired color intensity was achieved, embryos were fixed in 4%PFA for 20 minutes to inactivate the alkaline phosphatase. Embryos were visualized under Zeiss Discovery V8 pentafluor dissecting microscope and imaged using an Axiocam digital camera. Positive controls for the ISH protocol were a verified *Shh* riboprobe and the *Tom1* riboprobes on chick embryos overexpressing mouse *Tom1*. The negative control used was a sense *Tom1* riboprobe.

Vectastain Peroxidase Immunohistochemical Staining of Embryonic Spinal Cords and Adult Mouse Cerebellum:

For peroxidase staining of spinal cord sections, and adult mouse cerebellum Vectastain®ABC kit was utilized according to manufacturer's instructions (Vector Laboratories). Sections stored at -20° C were first permeabilized for 20 minutes in PBT. To quench endogenous peroxidase activity sections were incubated for 5 minutes (embryos) or 30 minutes (adult brain) in 0.3% H_2O_2. Slides were blocked and antibodies were diluted in normal horse serum/PBS and washes were done in PBT. Tom1 antibody or mouse IgG concentrations are indicated in Table 3. In order to visualize protein staining, liquid 3,3'-diaminobenzidine (DAB) and the substrate chromogen system (Dako Cytomation) was utilized according to manufacturer's instructions. Staining was allowed to develop until positive control slides (*mTom1*-electroporated chick spinal cords)

Table 3: Primary antibodies used in immunohistochemistry.

Antibody	Host	Dilution IHC	Source	Cat.#	Immunogen
Cleaved Caspase-3 (Asp175) (5A1E)	Rabbit	1/350	Cell Signaling	9664	Amino-terminal residues adjacent to Asp175 of Human Caspase-3
Mono or poly ubiquitinated proteins (FK2)	Mouse	1/500	Millipore	04-263	Poly-ubiquitinated-lysozyme
Nkx2.2	Mouse	1/50	Developmntal studies hybridoma bank	74.5A5	
Olig2	Guinea Pig	1/5000	Dr. B. Novitch		
Patched1 (G19)	Goat	1/250	Santa Cruz	sc6149	Peptide mapping to the N–terminus of Mouse Patched1
Pax6	Mouse	1/50	Developmental studies hybridoma bank	P3U1	Chick Pax6 a.a. 1-223
Rab7 (D95F2)	Rabbit	1/100	Cell Signaling	9367	Synthetic peptide corresponding to residues surrounding Glu188 of human Rab7 protein
Tom1	Mouse	1/5000	Abgent	AT4200a	Partial recombinant protein with GST tag (394a.a. to 492a. a. of human Tom1)

showed clear staining with low background. Sections were imaged on a Zeiss Axioplan II microscope and Axiocam HRC Color Camera using a 20X objective lens.

In Ovo Electroporation:

Fertilized chick eggs were incubated at 38°C two days prior to electroporation. Eggs containing HH stages 8-10 were windowed and visualized using India ink injected underneath the embryo. Plasmid DNA was purified using Quiagen Midiprep kit and kept as a concentrated sock (5μg/μl) in water. In order to transfect chicken embryonic neural tubes, fast green dye (50ng/μl) was added to the concentrated solution of DNA and injected into the lumen of the developing neural tube using a pulled glass capillary micropipette and aspirator assembly. Using a TSS20 Ovodyne Electroporator and EP21 Current Amplifier, a current was applied to either side of the neural tube (20-25V, 5 pulses, 50ms width, 500ms space) causing the plasmid DNA to enter cells on one side of the neural tube. The windowed eggs were subsequently sealed and returned to incubator for 24 hours. The embryos were dissected from extraembryonic tissues, fixed for 1 hour at RT in 4% PFA, rinsed in PBS, and equilibrated to 15% then 30% sucrose/PBS. Embryonic spinal cords were then oriented for transverse sections, embedded in OCT compound (Tissue Tek) and stored at -80°C until sectioned.

Immunohistochemistry of Ventral Progenitor Domains:

Embryonic spinal cords from electroporated embryos were sectioned at 12-14μm using a cryostat. Tissue was permeabilized for 20 minutes in PBT and blocked for 1h at RT in 5% donkey (DK) serum/PBS. Primary antibody (Table 3) was diluted in 5% DK

serum/PBS and incubated for 2 hours at RT or overnight at 4°C. Sections were washed three times in PBT and incubated in secondary antibody (Table 4) for 1 hour at room temperature while protected from light. Sections were then washed in PBT, counterstained with DAPI (Sigma, 1/5000 dilution of 3.3mg/mL stock) and coverslipped using Dako fluorescent mounting medium. Sections were stained with antibodies directed against transcription factors that specify various progenitor domains (Tables 3 and 4). Nkx2.2, Olig2 and Pax6 were used to visualize the p3, pMN and dorsal interneuron progenitors respectively, and appropriate secondary antibodies (Antibody dilutions Table 3 and Table 4). Immunostained sections were imaged using a Zeiss Axiovert 200M microscope and Hamatsu Orca R2 Camera using a 20X objective lens.

Analysis and Quantification of the Effect of Tom1 Overexpression in the Embryonic Spinal Cord:

In order to evaluate the effect of Tom1 overexpression on the electroporated versus contralateral control side of the embryonic spinal cord, a horizontal line was drawn along side the dorsal-most domain of a given progenitor marker on the unelectroporated side. More than one cell diameter change in progenitor domain (either ventrally or dorsally) was considered a shift. Embryos were excluded if the electroporated cells were not in progenitor domain in question. Thirty-six Tom1 electroporated embryos and 29 control plasmid electroporated embryo were used in evaluations. Up to two sections per embryo were evaluated for shifts in progenitor domains.

Table 4: Secondary antibodies used in immunohistochemistry.

Antibody	Host	Dilution IHC	Source	Cat.#
Alexa Fluor 555 Donkey Anti-mouse IgG (H+L)	Donkey	1/1000	Invitrogen	A-31570
Alexa Fluor 488 Donkey Anti-mouse IgG (H+L)	Donkey	1/1000	Invitrogen	A-21202
Alexa Fluor 647 Donkey Anti-mouse IgG (H+L)	Donkey	1/1000	Invitrogen	A-31571
Alexa Fluor 555 Donkey Anti-Goat IgG (H+L)	Donkey	1/1000	Invitrogen	A-21432
Alexa Fluor 488 Donkey Anti-Goat IgG (H+L)	Donkey	1/1000	Invitrogen	A-11055
Alexa Fluor 633 Donkey Anti-Goat IgG (H+L)	Donkey	1/1000	Invitrogen	A-21082
Alexa Fluor 555 Donkey Anti-Rabbit IgG (H+L)	Donkey	1/1000	Invitrogen	A-31572
Alexa Fluor 488 Donkey Anti-Rabbit IgG (H+L)	Donkey	1/1000	Invitrogen	A-21206
Alexa Fluor 647 Donkey Anti-Rabbit IgG (H+L)	Donkey	1/1000	Invitrogen	A-31573
Alexa Fluor 594 Goat Anti-Guinea Pig IgG (H+L)	Goat	1/1000	Invitrogen	A-11076

Culture of HEK293 Cells:

Human Embryonic Kidney (HEK)293 cells were cultured on 10 cm tissue culture dishes at 37°C in high glucose Dulbecco's Modified Eagle's Medium (DMEM; Gibco), 10% heat inactivated fetal bovine serum (HI-FBS), L-glutamine (2mM), and Pen-strep (100units/mL penicillin, 100ug/mL streptomycin) until 60-80% confluency was reached and were passaged at 1 in 6 to 1 in 10.

Western Blot Procedures:

Sodium dodecyl sulphate (SDS) polyacrylamide gel electrophoresis was conducted using a Bio-Rad Mini-PROTEAN apparatus and 6% or 7.5% polyacrylamide gels. Gels were run at 125V then electrobloted to polyvinylidene difluoride (PVDF) membrane at 110V for 1 hour.

Transfection of HEK293 cells for Co-immunoprecipitation and Subcellular fractionation:

50µl polyethylenimine (PEI; 2mg/mL) + 15µg plasmid DNA was added to 1mL of high glucose DMEM and incubated for 10 minutes at RT. Mixture was then added drop-wise to a 10 cm tissue culture plate containing 60% confluent HEK293 cells and incubated for 12-24 hours. Cells were transfected with pRK5 mPtch1-Myc, pcDNA5/FRT Flag-Ptch1^{Wig},pIRES2-EGFP Tom1 or pcDNA3.1(+) Tom1 (Table 1).

Co-immunoprecipition of Tom1 and Patched1^{Wiggable}:

HEK293 cell lines stably expressing Flag-tagged Ptch1^{Wig} (two independent lines 1A and 2) or wild-type HEK293 cells were lysed in IP lysis buffer (0.5% NP-40, 150mM NaCl, 20mM Tris-Cl, 1mM EDTA, protease inhibitor (Sigma)) and immunoprecipitated using Sigma Flag IP Kit. Sample buffer (63mM Tris pH 6.8, 1% glycerol, 6.4% SDS, 0.5% 2-ME, 0.25% Bromophenol blue) was added to 20 µl of Flag purified cell lysate and separated on a 7.5% SDS polyacrylamide gel, transferred and blocked for 1 hour in 5% milk/Tris-buffered saline with 0.1% Tween-20 (TBST). Tom1 antibody (Table 5) was incubated overnight at 4°C on a nutating platform. The next day, the membrane was rinsed three times in TBST and incubated for 2h at RT in secondary antibody (Table 6). The membranes were rinsed three more times in TBST and visualized using Pierce electrochemiluminescence (ECL) 2 kit. To verify Ptch1^{Wig} was immunoprecipitated, the blot was stripped using Restore Stripping buffer (Pierce) for 15 minutes, rinsed for 1-3 hours in TBST and re-probed for Ptch1 and Flag using antibodies outlined in (Table 5 & 6).

Co-immunoprecipition of Tom1 and Wild-type Ptch1:

Wild-type HEK293 cells were transfected with Myc-tagged wild-type *Ptch1* (Table 1), either singly or with *Tom1* pIRES2-EGFP using Fugene 6 reagent from Promega (50µl of Fugene 6 + 17µg of plasmid DNA). Cells were lysed 24 hours after transfection in 1mL of IP lysis buffer (0.5% NP-40, 150mM NaCl, 20mM Tris-Cl, 1mM EDTA, protease inhibitor) and incubated for 30 minutes at 4°C while rocking. Cells were then centrifuged at 12,000 rpm for 15 minutes at 4°C and 500µl of supernatant was

Table 5. Primary antibodies used in Western Blots.

Antibody	Host	Dilution WB	Source	Cat.#	Immunogen
Tom1	Mouse	1/5000	Abgent	AT4300a	Partial recombinant protein with GST tag (394a.a. to 492a. a. of human Tom1)
Myc-Tag (9B11)	Mouse	1/1000	Cell Signaling	2276	Synthetic peptide corresponding to residues 410-419 of human c-Myc
DYKDDDDK (Flag) Tag Antibody	Rabbit	1/1000	Cell Signaling	2368	Synthetic peptide DYKDDDDK
Flag M2	Mouse	1/1000	Sigma	F1804	Synthetic peptide DYKDDDDK
αTubulin	Mouse	1/1000	Sigma	T9026	Microtubules from chicken embryo brain
Patched1 (G19)	Goat	1/1000	Santa Cruz	Sc6149	Peptide mapping to the N–terminus of Mouse Patched1

Table 6: Secondary Antibodies used in Western Blots.

Antibody	Host	Dilution WB	Source	Cat #
HRP conjugated Donkey anti-mouse IgG	Donkey	1/10000	Pierce Thermoscientific	PA-28748
HRP conjugated Goat anti-mouse IgG	Goat	1/10000	Pierce Thermoscientific	31430
HRP conjugated Rabbit anti-goat IgG	Rabbit	1/10000	Pierce Thermoscientific	31402
HRP conjugated Donkey anti-Rabbit IgG	Donkey	1/10000	Pierce Thermoscientific	31458

immunoprecipitated for wild-type Ptch1 using Pierce C-Myc immunoprecipitation kit. Beads (10µl) were added to lysates and incubated overnight at 4°C. In the morning, beads were washed in TBST (0.5% Tween-20) three times and eluted with 25µl of 2X sample buffer. All 25µl of eluted protein was loaded on SDS 7.5% polyacrylamide gel and transferred to a PVDF membrane. Membrane was blocked in 5% milk/TBST and probed with Tom1 and Myc antibodies (Table 5) overnight at 4°C. The next day the membrane was washed in TBST, incubated in horseradish peroxidase (HRP) secondary antibody (Jackson Immunoresearch; Table 6) for 2 hours, and visualized using Pierce ECL 2 kit.

Sub-cellular Fractionation of Transfected HEK293 cells.

In order to obtain sub-cellular fractions of HEK293 cells expressing Tom1 and Ptch1, the following protocol was adapted from Lallemand et al., 2003 and depicted in Figure 8. Transfected cells were rinsed twice in PBS and incubated in 1mL of hypotonic buffer (10mM HEPES (pH7.4)/1mM EDTA/ protease inhibitors) on ice for five minutes. Cells from 2 plates were scraped and pooled, and homogenized using a Dounce homogenizer. Subsequently, homogenized cells were centrifuged at 600g for 10 minutes at 4°C. The supernatant was transferred to another tube and the pellet was redissolved in 1mL of hypotonic buffer and both the supernatant and redissolved pellet were centrifuged as above. The supernatant was transferred to a new tube and put aside on ice while the supernatant from pellet was discarded. The pellet was redissolved again in 1mL of hypotonic buffer and centrifuged at 15,000g for 10 minutes. The resulting supernatant was discarded and the remaining pellet was resuspended in 500µl of RIPA buffer (50mM

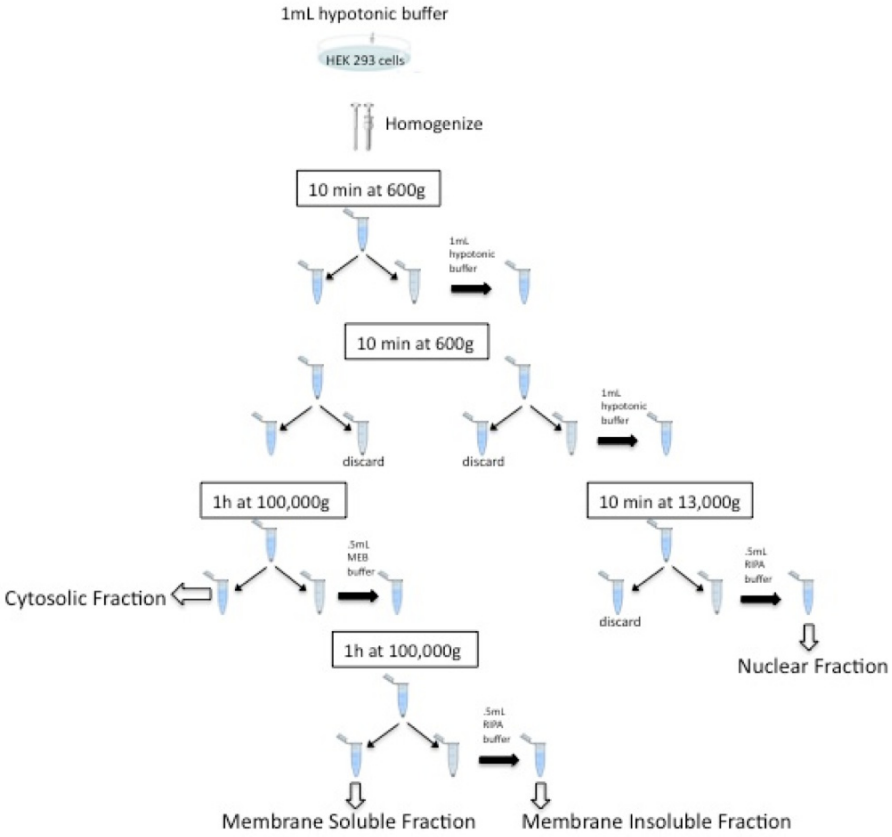

FIGURE 8. Diagram of Subcellular Fractionation Method. (Lallemand et al. 2003). After each centrifugation the pellet and supernatant are separated and the pellet either discarded or resuspended in buffer (solid arrow), the supernatant is either discarded or centrifuged further. The centrifugation steps are indicated in boxes.

Tris (pH7.4)/ 1% TritonX100/0.1% SDS/0.5% sodium deoxycholate/150mM NaCl/1mM EDTA/protease inhibitors) to give the nuclear fraction.

The supernatant was then ultracentrifuged for 1h at 100,000xg at 4°C to give the cytosolic fraction (supernatant) and membrane fraction (pellet). The membrane fraction was then dissolved in 500µl of membrane extraction buffer (MEB) buffer (50mM Tris (pH 7.4)/1% TritonX100/150mM NaCl/1mM EDTA/Protease Inhibitors) and centrifuged again for 1h at 100,000g to give the membrane soluble fraction (supernatant) and membrane insoluble fraction (pellet). The membrane insoluble fraction was then dissolved in 500µl of RIPA buffer. The protein content of all fractions was measured using a protein assay kit (Pierce BCA Protein Assay Kit) and normalized by dilution with appropriate buffer. Sample buffer (5X) was added and incubated at RT for 15 minutes before loading on SDS polyacrylamide gel. Protein from each fraction was assayed using Western blot and was immunostained for Tom1 and Ptch1 as described above.

Transfection of HEK293 Cells for Immunofluorescence:

HEK293 cells (60,000/16mm well) were plated 24h before transfection on Poly-D-lysine coated glass coverslips nested at the bottom of a 24 well plate. The following day 1.5µl of Fugene 6 (Promega) or PEI (2mg/mL) and 0.5µg of plasmid DNA were diluted in 25µl of high glucose DMEM per well. The mixture was incubated 10 min at RT then added drop-wise to cells and incubated for 4-24 hours at 37°C. After transfection, cells were washed in PBS, fixed in 4% PFA for 10 minutes, and rinsed three times in PBS.

Immunohistochemistry of HEK293 cells:

Cells were permeabilized for 20 minutes in PBT and blocked for 1h at RT in 5% DK serum/PBS. Primary antibody (Table 3) was diluted in 5% DK serum/PBS and incubated for 2 hours at RT or overnight at 4°C. Cells were washed three times in PBS and incubated in secondary antibody (Table 4) for 1 hour at RT while protected from light. Cells were washed in PBS, counterstained with DAPI (Sigma, 1/5000 dilution of 3.3mg/mL stock), and post-fixed in 4% PFA for 10 minutes. Cells were imaged on a Zeiss LSM 510 Meta Laser Scanning Confocal Microscope using 63X or 40X objective lenses. In order to rule out bleed through in co-localization experiments, antigens were visualized using the secondary dyes Alexa Fluor 488 and Alexa Fluor 647, which have virtually no overlap in emission spectra. Omission of primary antibody was used as a negative control.

Analysis of Tom1 and Ptch1 Aggregate Formation.

Ptch1 both alone and with Tom1 was transfected and immunostained for Ptch1 and Tom1 as described above. Cells were imaged at 63X using a Zeiss Axiovert 200M microscope and Hamatsu Orca R2 Camera. 100 transfected cells from 3 different slides per condition were assessed for the presence of an aggregate. Aggregates were defined as a large circular collection of protein at the perinuclear region that stains considerably more intensely than the rest of the protein in the cell. A comparison between groups was made using a two-tailed student's t test.

CHAPTER 3: RESULTS

An interesting feature of Sonic hedgehog (Shh) signaling is that the receptor for Shh proteins, called Patched1 (Ptch1), is both a negative regulator and transcriptional target of the pathway. This implies that Ptch1 limits both the spread of extracellular Shh, and intracellular Shh signaling over time. Given the key role for Ptch1 in regulating the extent of Shh signaling, it is crucial that we explore the mechanism that regulates the localization and dynamics of Ptch1 within the cell as the levels and localization of Ptch1 will ultimately affect how cells receive and interpret the Shh signal.

Ptch1 is internalized by dynamin-mediated endocytosis and is targeted to lysosome for degradation (Incardona et al, 2000; 2002). Furthermore, intact endocytic cycling of the Ptch1-Shh complex is required for downstream Shh signaling in vertebrate cells (Incardona et al. 2002). However, the regulation of Ptch1 subcellular localization and degradation is poorly understood.

Given that there are very few known regulators of Ptch1 endocytic cycling and degradation, our group conducted a proteomic screen to identify novel genes that are involved in this process (unpublished findings). The proteomic screen was conducted using the N-terminal portion (amino acids 1-848) of the Ptch1 protein called Patched 1 Wiggable ($Ptch1^{Wig}$). This segment was used because it allowed for the creation of a cell line that stably expresses $Ptch1^{Wig}$. Full length Ptch1 is an apoptotic inducing protein; therefore, creation of a stable cell line expressing the entire protein was not feasible (Thibert et al., 2003; Fombone et al., 2012). Flag-tagged $Ptch1^{Wig}$ was immunoprecipitated and subjected to mass spectrometry to identify interacting proteins. One of the proteins identified was target of myb1 (Tom1), which is an adapter protein

involved in endocytic cycling thought to target ubiquitinated proteins to the lysosome (Wang et al., 2010). Given that Ptch1 is ubiquitinated and is degraded through the lysosome we reasoned that Tom1 might have a role in Ptch1 endocytic cycling and/or degradation.

Tom1 Co-immunoprecipitates with Ptch1^{Wig} but not Wild-Type Ptch1.

To rule out the possibility that the Tom1-Ptch1^{Wig} interaction found by mass spectrometry was a false positive, the interaction between Ptch1^{wig} and Tom1 was confirmed by co-immunoprecipitation (Figure 9A). Flag-Tagged Ptch1^{Wig} stable cell lines were lysed and immunoprecipitated for Flag using anti-Flag immobilized agarose beads. Immunoprecipitated lysates were then probed for the presence of Tom1 using a monoclonal antibody (Abgent). Endogenous Tom1 was found to co-immunoprecipitate with Ptch1^{Wig} in two separate Ptch1^{Wig} human embryonic kidney (HEK293) cell lines that both stably express Ptch1^{Wig} (Lines 1a and 2; Figure 9A). Tom1 was absent in wild-type HEK293 cells undergoing the same procedure (Figure 9A). Tom1 was found at the expected size of 54kD (Figure 9A). However, another band was also detected by the Tom1 antibody at 33 kD. It is unclear what this band represents, but this finding is consistent with reports from other groups using an antibody against tagged Tom1 (Katoh et al., 2004).

To determine if Tom1 interacts with full length Ptch1, Myc tagged wild-type Ptch1 and Tom1 were overexpressed together in wild-type HEK293 cells. Cells were lysed and Myc tagged Ptch1 was immunoprecipitated using anti-Myc immobilized beads

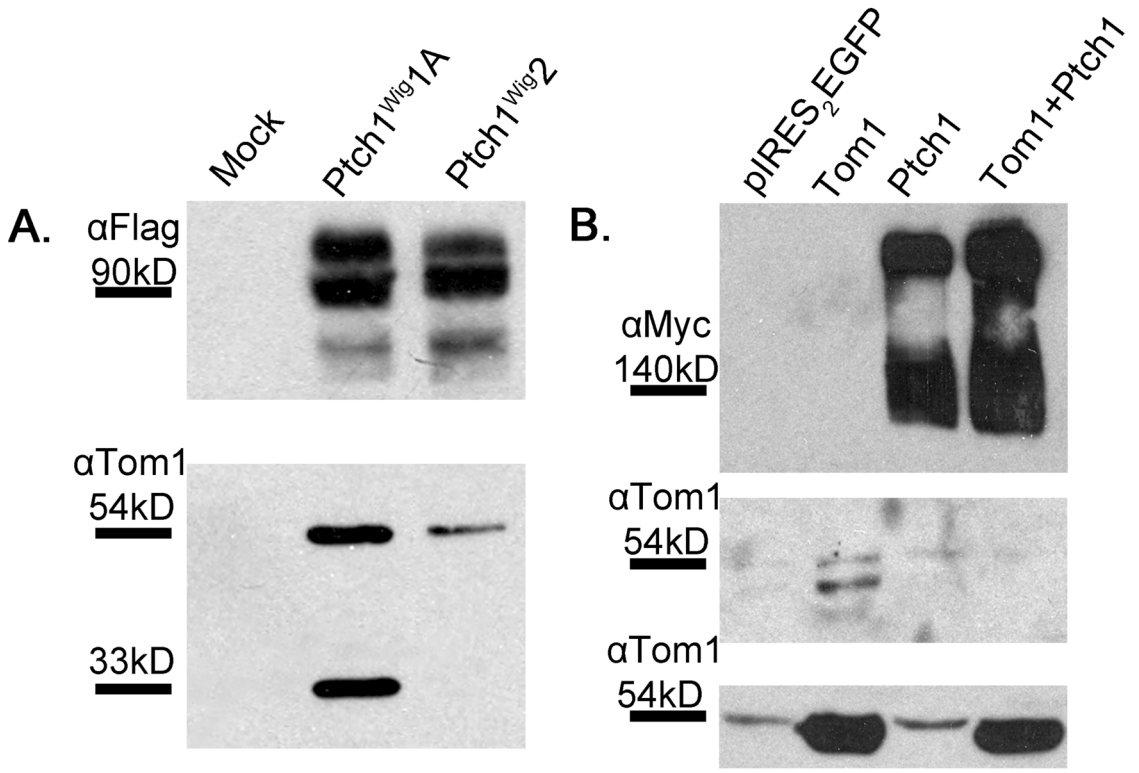

FIGURE 9. Tom1 associates with the N-terminus of Patched1 (Ptch1). (A) Endogenous Tom1 co-immunoprecipitates with two different lines of Flag-tagged $Ptch1^{Wig}$ (Lines 1A and 2). Top panel shows Flag immunoprecipitated $Ptch1^{Wig}$ at 90kD. Bottom panel shows immunoprecipitated Tom1 at 54kD and the presence of another band of unknown origin at 33kD. (B) Tom1 did not immunnoprecipitate with Myc-purified wild-type Ptch1 in transfected HEK293 cells. Top panel shows immunoprecipitated lysates stained for Myc at 150kD. Middle panel shows immunoprecipitated lysates stained for Tom1. Bottom panel shows whole cell lysates 5% of immunoprecipitated input stained for Tom1.

and probed for Tom1. Neither overexpressed nor endogenous Tom1 was detected in immunoprecipitated lysates (Figure 9B). Very low levels of endogenous Tom1 (upper band) were found in all conditions indicating that Tom1 did not co-immunoprecipitate with wild-type Ptch1 under our conditions (Figure 9B).

Analysis of Tom1 mRNA Expression in the Developing Chick and Mouse Embryo.

Given that Tom1 associated with the amino-terminus of Ptch1, and its embryonic expression profile is unknown, Tom1 expression was evaluated to determine if it was expressed in the same tissues as Ptch1 during nervous system development. The LacZ knock-in Ptch1 locus was used to visualize the tissues that express the Ptch1 gene during neural development. LacZ staining reveals at E9.5 Ptch1 is expressed throughout the developing neural tube in a gradient with high levels ventrally and lower levels dorsally (Figure 10).

The mRNA expression pattern of *Tom1* in the developing embryo was investigated in regions of Ptch1 expression. To determine if *Tom1* mRNA was expressed in the developing mouse embryo, mRNA was first extracted from mouse E10.5 whole embryo lysates and reverse transcriptase polymerase chain reaction (RT-PCR) was conducted using primers designed for *Tom1* cDNA (Table 1). Mouse *Tom1* mRNA was detected in E10.5 mouse embryos (Figure 11D).

To determine where *Tom1* mRNA was expressed in the developing embryo, whole embryo *in situ* hybridization was conducted. *Tom1* mRNA was not detected by *in situ* hybridization at high levels in any specific structures in the E8.5, E9.5 and E10.5 mouse embryo or E3.5 chick embryo (Figure 11, 12). Furthermore, *Tom1 in situ*

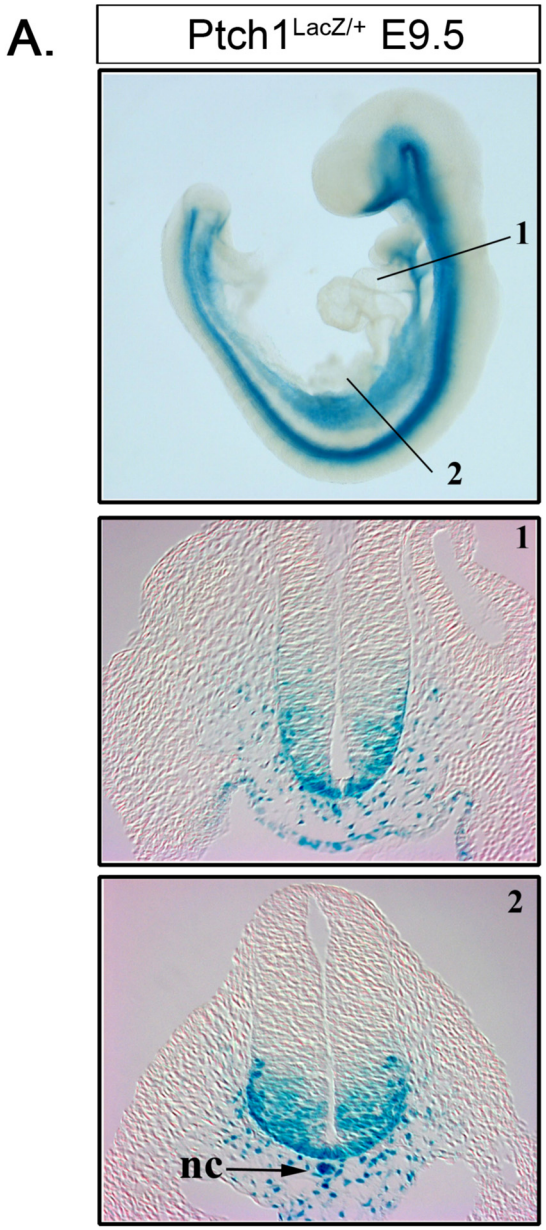

FIGURE 10. Ptch1 activity during neural development. (A)*Top panel*: Lateral view of LacZ whole mount staining of an E9.5 Ptch1$^{Lacz/+}$ embryo. LacZ staining shows Ptch1 expression in the whole E9.5 embryo throughout the entire length of the developing central nervous system. *Middle and bottom panels*: Transverse sections across the cervical (1) and forelimb bud (2) regions show the ventral-high gradient of Ptch1, reflecting tissues responding to Shh signaling. Abbreviations: nc, notochord. Figure supplied by Dr. Angelo Iulianella.

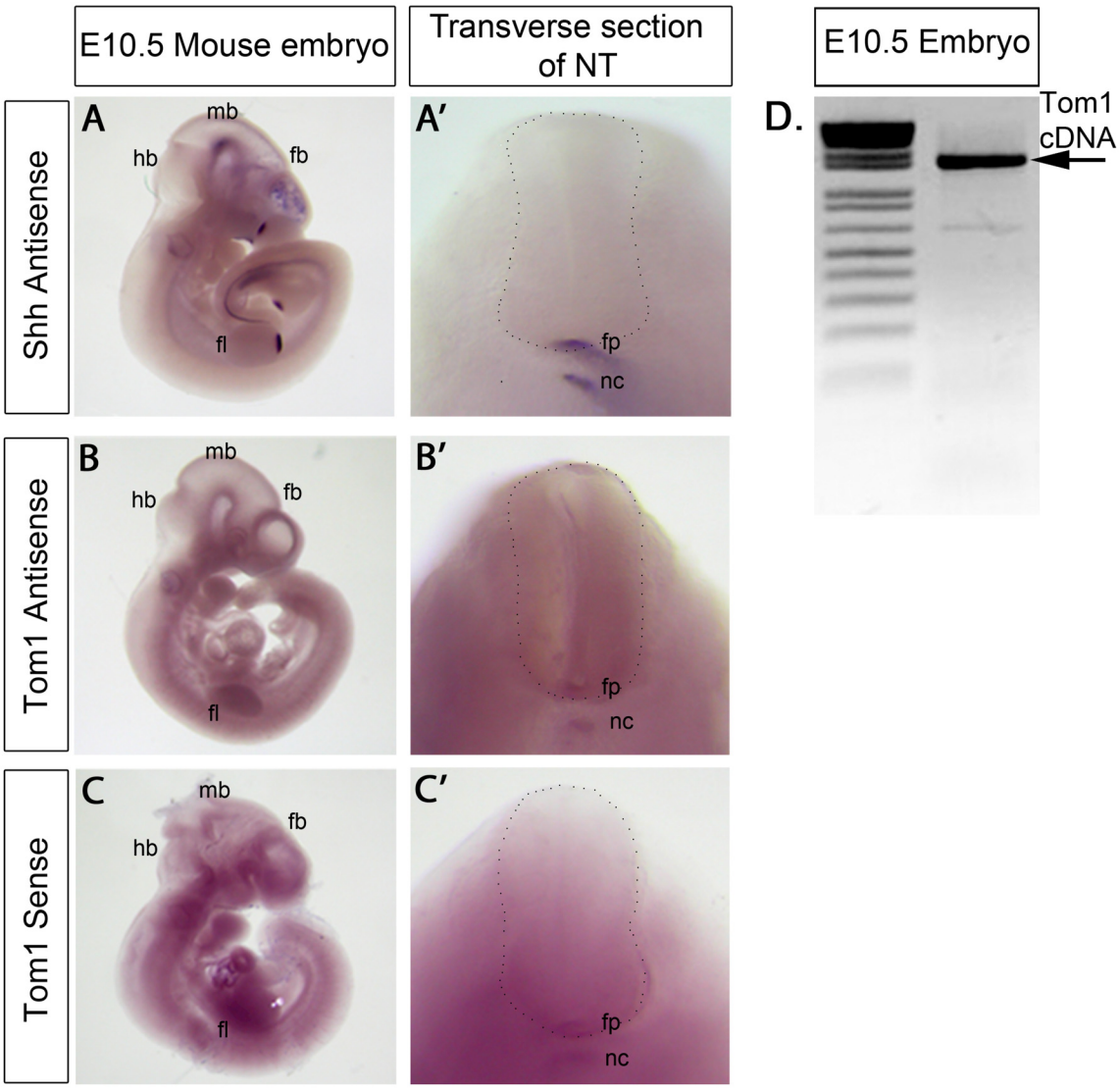

FIGURE 11. Tom1 and Shh mRNA expression in the E10.5 mouse embryo. (A) Lateral view of an E10.5 embryo stained with *Shh* antisense riboprobe. (B) Lateral view of an E10.5 embryo stained with *Tom1* antisense riboprobe. (C) Control *Tom1* sense riboprobe in an E10.5 embryo. (A'-C') Transverse sections of embryos at forelimb bud probed for *Shh*, (A'), *Tom1* antisense (B'), and *Tom1* sense (C') riboprobes. (D) RT-PCR of E10.5 total mRNA using primers against Tom1 confirms embryonic expression. Abbreviations: (hb) hindbrain, (mb) midbrain, (fb) forebrain, (fl) forelimb bud, (fp) floorplate, (nc) notochord.

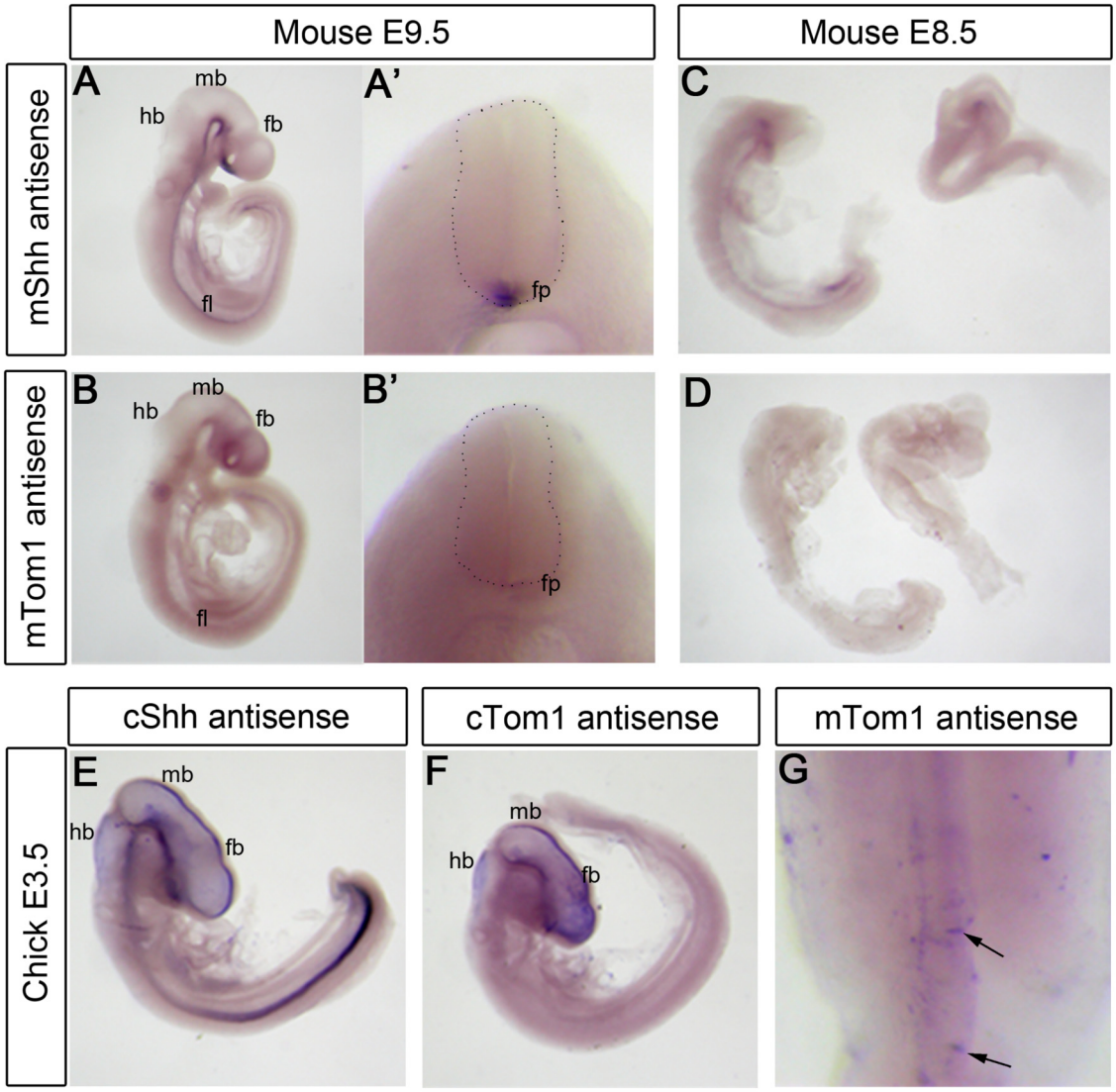

FIGURE 12. Comparative expression profile for Tom1 and Shh in early mouse and chick embryos. (A, B) Lateral view of a mouse E9.5 embryos hybridized with *mShh* (A) and *mTom1* (B) riboprobes. (A' and B') Transverse section of neural tube in A and B at the limb bud. Lateral view of E8.5 mouse embryos hybridized with *mShh* (C) or *mTom1* (D) riboprobes. (E and F) Lateral view of chick E3.5 embryo hybridized with cShh (E) or *cTom1* (F) riboprobes. (G) Dorsal view of E3.5 chick neural tube electroporated with *mTom1* expressing plasmid and hybridized with mTom1 riboprobe. Arrows indicate *mTom1* mRNA positive cells following electroporation. Forebrain (fb), midbrain (mb), hindbrain(hb), forelimb bud(fl), floorplate(fp).

hybridization did not reveal high levels of expression in the neural tube (Figure 11B', Figure 12B'). However staining in the neural tube did appear to be slightly higher for *Tom1* mRNA than the sense control in the E10.5 embryo. Mouse and chick *Tom1* riboprobes showed similar ambiguous results for *Tom1* in developing neural tissues.

Two separate mouse *Tom1* mRNA probes that hybridize to different sections of the mouse *Tom1* gene and one chick *Tom1* mRNA probe were used for hybridization (Figure 7). A *Tom1* sense mRNA probe was used as a negative control for E10.5 embryos and mRNA probes against mouse and chick *Shh* were used as a positive controls for all stages of embryos (Figure 11A, C; Figure 12A, C, E). The mouse *Tom1* riboprobes were verified by performing *in situ* hybridization on electroporated chick embryos overexpressing mouse *Tom1* in the neural tube (Figure 12G). The *Tom1* mouse mRNA probe detected electroporated cells confirming that the probe detects *Tom1* mRNA under our experimental conditions (Figure 12G, arrows).

Tom1 Protein is Expressed in the Mouse Embryo and in the Adult Cerebellum.

Given that the *Tom1* mRNA expression pattern was inconclusive, Tom1 protein distribution in the developing nervous system was investigating using a commercial antibody. Endogenous Tom1 was stained using a monoclonal antibody against Tom1 (Abgent; Table 3 and 5). Tom1 protein was detected in E10.5 whole embryo lysates by Western blot indicating that it was expressed in the embryo (Figure 13D).

To determine the distribution of Tom1 in the developing spinal cord, transverse sections of mouse E9.5 neural tube were immunostained using a horse radish peroxidase (HRP) amplification and detection kit and compared to control sections stained with the

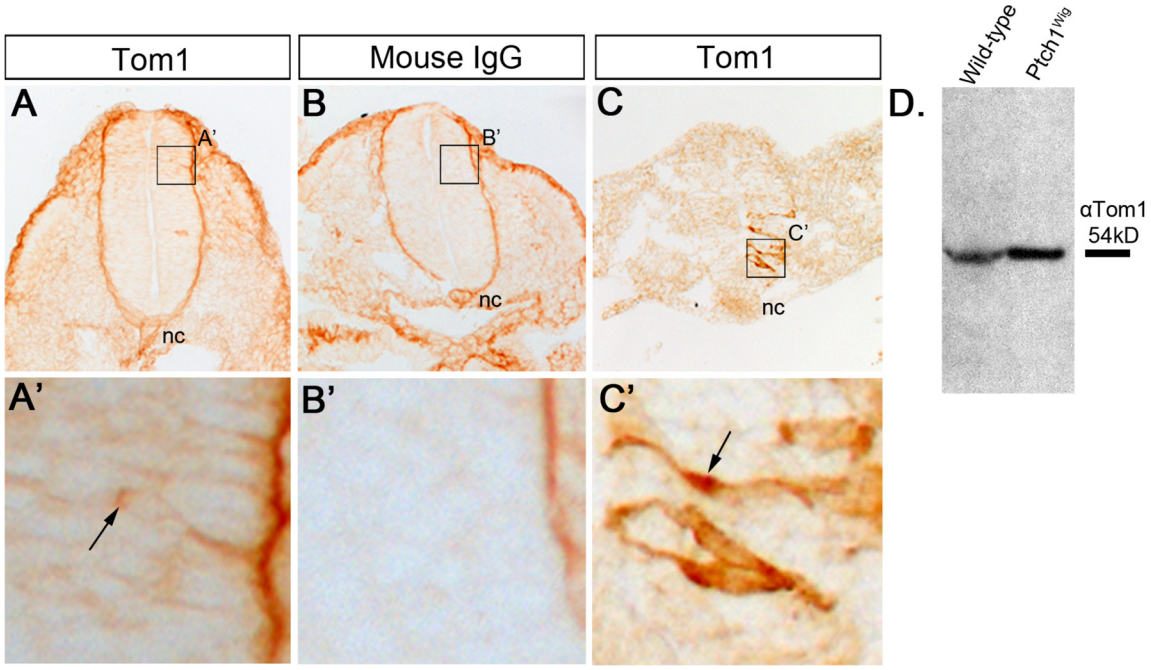

FIGURE 13. Tom1 protein expression in the embryonic spinal cord. (A, A') Tom1 immunohistochemistry on transverse sections of mouse E9.5 spinal cords. Tom1 showed a cytoplasmic localization (A' arrow). (B ,B') Mouse IgG negative control. (C, C') Tom1 staining in mTom1 electroporated chick E3.5 spinal cords (24 hours post-electroporation; arrow in C'). (D) Western blot for Tom1 protein in E10.5 wild-type and Ptch1^{Wig} whole embryo lysates. Notocord (nc).

same concentration of mouse IgG (Figure 13A-B). Tom1 protein was detected in the mouse embryonic spinal cord at E9.5, with slightly higher expression in the dorsal half of the neural tube. Tom1 protein was found throughout the cytoplasm, consistent with the pattern that was also observed when overexpressed in the chick neural tube (Figure 13A', arrow). Control mouse IgG staining did not reveal any positive cells within the neural tube. Transverse sections of electroporated chick E3.5 spinal cords overexpressing mouse Tom1 were used as a positive control (Figure 13C). Interestingly, the expression pattern in the neural tube of Tom1 was inversely correlated to *Ptch1* activity levels, which are high in ventral neural tissues. The *Ptch1* LacZ transgenic mouse is a read-out for Shh signaling because Ptch1 is a target of the pathway. Thus, the inverse correlation of Tom1 protein expression with Shh activity suggests that Tom1 may be involved in controlling the extent of Shh signaling in target cells in the developing nervous system.

Tom1 was previously reported by the Human Protein Atlas to be highly expressed in the human adult cerebellum (http://www.proteinatlas.org/ENSG00000100284/normal). Shh signaling is extremely important for development of the cerebellum and Shh components continue to be expressed in the adult cerebellum (Petralia et al. 2012). The adult cerebellum can be subdivided into three distinct layers: The molecular cell layer, the Purkinje cell layer and the granular cell layer. A recent study found that Ptch1 is expressed in Purkinje cells, granule cells and molecular layer interneurons of the adult rat cerebellum (Petralia et al., 2012). Furthermore, Ptch1 is associated with the postsynaptic dendritic spines of neurons, localizing to cell surface, and endosomes (Petralia et al., 2012). Tom1 expression in the adult cerebellum was confirmed using immunohistochemistry (Figure 14A). Tom1 was located in the Purkinje cells and in

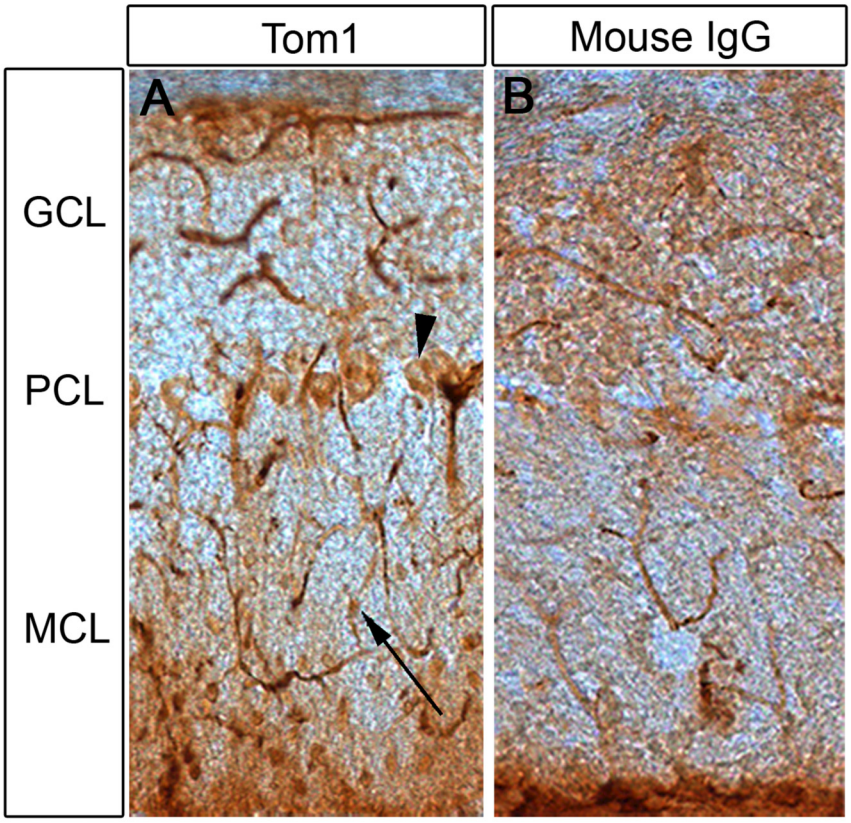

FIGURE 14. Tom1 protein expression in the adult mouse cerebellum. (A) Tom1 immunostaining of the adult mouse cerebellum. Tom1 localizes to Purkinje cells (arrowhead) and interneurons of the MCL (arrow). (B) Control Mouse IgG immunostaining. Abbreviations: GCL, Granular cell layer; PCL, Purkinje cell layer; MCL, molecular cell layer.

interneurons of the molecular layer (Figure 14A, arrowhead, arrow). Consistent with expression in the neural tube, Tom1 had a cytoplasmic localization. These results confirm the presence of Tom1 in two regions of Ptch1 expression: the developing neural tube and the adult cerebellum.

Tom1 Does Not Affect Dorso-Ventral Patterning of the Chick Neural Tube.

Given that Tom1 interacts with $Ptch1^{Wig}$ and its expression pattern overlaps with Ptch1 in the mouse, a functional role for Tom1 in Shh signaling through its interaction with Ptch1 was investigated. The ventral neural tube has well-defined progenitor domains arranged along the ventral-to-dorsal axis that differentiate in response to graded Shh (Figure 1). Overexpression of genes affecting Shh signaling at stages when these domains are being established also affects the development of these discrete progenitor domains (Briscoe et al., 2001; Stamataki et al., 2005). Overexpression of a Ptch1 mutant that cannot bind Shh but still can inhibit smoothened (Smo; $Ptch1^{\Delta Loop2}$) causes a down regulation of Nkx2.2 and ventral expansion of Pax6 in the developing chick spinal cord (Briscoe et al., 2001). Furthermore, overexpressing growth arrest-specific protein 1 (Gas1), which is a facilitator of Shh signaling, expands the Nkx2.2 progenitor domain (Martinelli & Fan, 2007). Therefore, the chick neural tube is a useful system to functionally assess the effect of any given gene on Shh signaling.

To assess if Tom1 plays a functional role in Shh signaling Tom1 was overexpressed on one side of the chick neural tube (HH stages 8-11). At this stage, neural progenitor domains are being established in the chick embryo. Therefore it is an ideal time to test the ability of a candidate factor to alter Shh signaling dependent progenitor

development. To do this, a bicistronic plasmid expressing both Tom1 and enhanced green fluorescent protein (EGFP; to monitor transfection efficiency) was injected into the lumen of the neural tube and the embryo was electroporated. This caused the construct to be expressed in cells on one side of the neural tube allowing for an internally controlled comparison of progenitor domains between the electroporated and unelectroporated sides. The effect of Tom1 overexpression on progenitor domain populations induced by Shh signaling was evaluated by examining motoneuron progenitors with an antibody against Olig2, and V3 interneuron progenitors by an Nkx2.2 antibody. If Tom1 is a negative regulator of Ptch1, it is expected it would have a positive effect on Shh signaling and cause a dorsal shift in ventral progenitor domains inducted by Shh.

Tom1 overexpression caused a dorsal shift in both the Nkx2.2 (45%, n=31) and Olig2 (45%, n=40) ventral progenitor domains compared to the unelectroporated side (Figure 15). A shift was defined as a change in more than one cell layer in the progenitor domain compared to the unelectroporated side. However, this effect was also observed, although to a lesser extent, in control embryos electroporated with a construct only expressing EGFP (Nkx2.2 27% n=22; Olig2 37% n=30). Figure 15 shows examples of experimental and control embryos without a shift and with a shift in Nkx2.2 and Olig2 progenitor domains.

Pax6 is a transcription factor that is expressed throughout the neural tube outlining ventral interneuron progenitors V0-V2. It is excluded from the Nkx2.2-positive V3 progenitors. Pax6 is expressed in a gradient, with low levels ventrally and high levels dorsally, and its expression is repressed by high levels of Shh (Ericson et al., 1997).

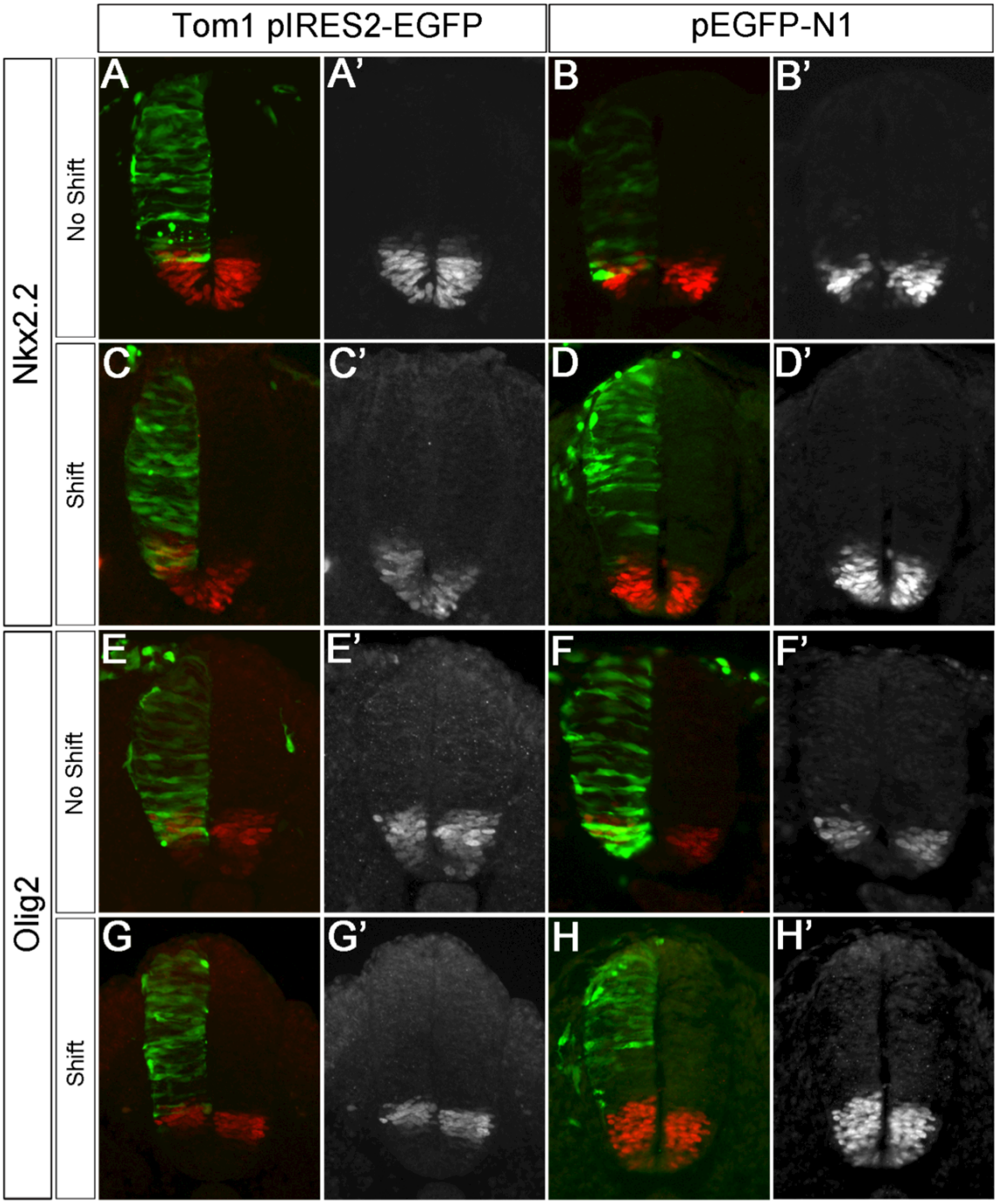

FIGURE 15. Functional in vivo assay for Tom1 in Shh-mediated spinal cord patterning. Transverse sections of E3.5 chick embryonic spinal cords 24 hours post-electroporation immunostained for p3 progenitor marker Nkx2.2 and pMN progenitor marker Olig2. (A-D) Nkx2.2 p3 staining (red) following Tom1pIRES2-EGFP (A, A', C, C') overexpression vs. control pEGFP-N1 control electroporations (B, B', D, D'). Progenitor marker signal is shown as red in merge images with GFP transfected spinal cords and as black and white images to reveal shifts. (E-H) Olig2 pMN staining (red) following Tom1pIRES2-EGFP (E, E', F, F') overexpression vs. control pEGFP-N1 control electroporations (G, G', H, H').

Therefore Pax6 is expressed in a graded fashion to differing levels of Shh. This makes it an excellent candidate to assess genes that may have a positive effect on Shh signaling, as its expression may be more susceptible to fluctuations in Shh signaling than the Nkx2.2- and Olig2-progenitor domains. Therefore the effect of Tom1 electroporation on Pax6 expression in the neural tube was evaluated. Both EGFP and Tom1 overexpression caused a repression of Pax6 in the ventral chick neural tube. However, this effect was only observed in 24% (n=17) of Tom1 electroporated embryos and 20% (n=15) of EGFP electroporated embryos (Figure 16). Figure shows examples of normal Pax6 expression and Pax6 repression on the electroporated side of the embryo. Therefore, overexpression of Tom1 was not found to have a consistent effect on Pax6 expression in the chick embryo.

Tom1 and Ptch1 Co-localize when Co-expressed in Cell Culture

Tom1 overexpression was not found to have an effect on dorsal-ventral patterning of the chick neural tube, however overexpression of Tom1 alone may not be sufficient to induce a functional consequence on downstream Shh signaling. Alternatively Tom1 may regulate Ptch1 in other tissues besides the developing neural tube. To investigate these two possibilities we used a cell culture model system to explore the nature of the interaction between Ptch1 and Tom1. To do this we used HEK293 cells, as they are easily transfected, well-suited for co-immunoprecipitation studies, and were used to obtain the proteomic data that that implicated an interaction between Ptch1 and Tom1.

Previous studies overexpressing Ptch1 have reported that Ptch1 is constitutively endocytosed and co-localizes with Rab7 positive vesicles (Incardona et al., 2000, 2002;

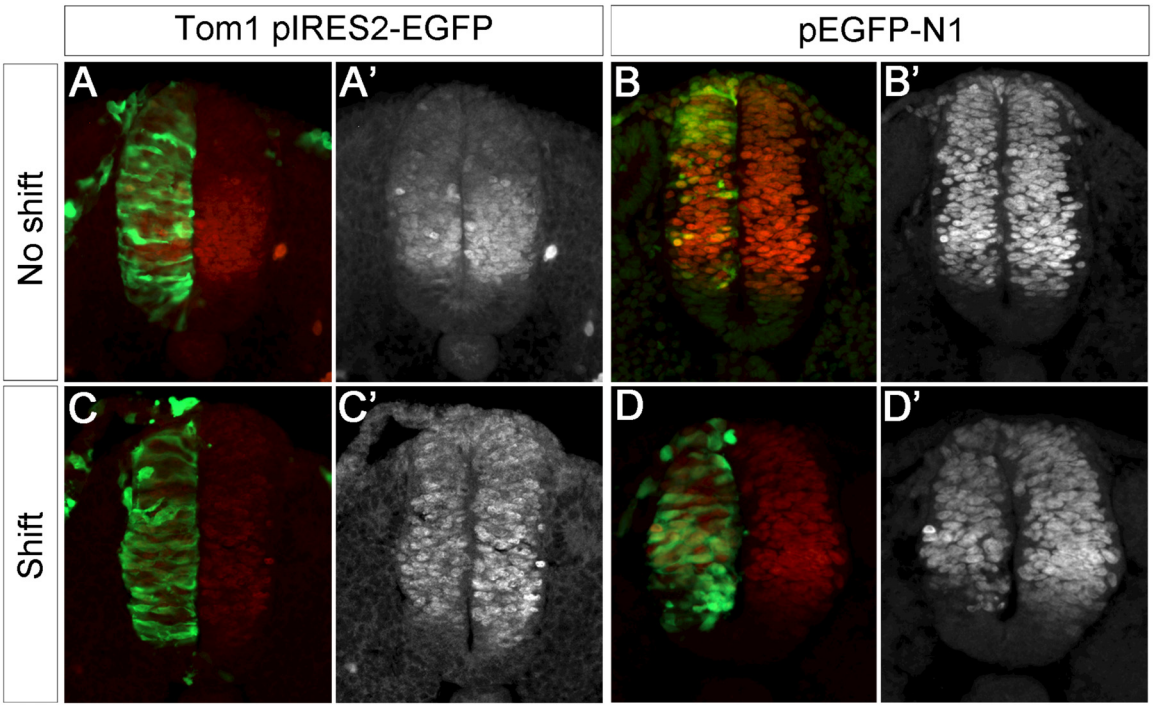

FIGURE 16. Tom1 electroporation did not affect specification of the Pax6 progenitor domain. Transverse sections of E3.5 chick embryonic spinal cords 24 hours post-electroporation immunostained for interneuron progenitor marker Pax6. (A-D) Pax6 immunostaining (red) in Tom1pIRES2-EGFP (A, C) and pEGFP-N1 electroporation spinal cords (B, D). Tom1pIRES2-EGFP and pEGFP-N1 electroporation (B, C) either had no effect on Pax6 progenitor domain (A' and B') or produced dorsal contraction in Pax6-positive cells on the electroporated side (C' and D').

Gallet and Therond, 2005; Callejo et al., 2007). In order to ensure Ptch1 behaves the same way in HEK293 cells, Ptch1 was transfected and cells were immunostained for both Ptch1 and Rab7. Ptch1 and Rab7 co-localized in small punctae, verifying our expression system (Figure 17, arrows).

To determine if Tom1 and Ptch1 could be found in the same compartment in the cell a subcellular fractionation was conducted. Wild-type Ptch1 alone or with Tom1 was overexpressed in HEK293 cells. Cells were then lysed and subjected to a subcellular fractionation. Fractionation of cells revealed that Ptch1 is present in both the membrane soluble and insoluble fractions while Tom1 is present in the cytoplasmic and membrane soluble fractions (Figure 18A). Co-expression of Tom1 and Ptch1 did not change the distribution of Ptch1 in each fraction.

Since both Ptch1 and Tom1 were found in the membrane soluble fraction, the subcellular localization of Tom1 and Ptch1 was investigated in cultured HEK293 cells using immunofluorescence. Plasmids expressing Tom1 and Ptch1 were transfected, immunostained, and visualized using confocal microscopy. First, the subcellular distribution of wild-type Ptch1 transfected alone was evaluated. When transfected alone Ptch1 localized to punctate structures throughout the cell and concentrated at the perinuclear region (Figure 17A &18C).

In contrast, when Tom1 was overexpressed alone it was found throughout the cytoplasm of the cell and occasionally in punctate structures, consistent with previous reports of overexpressed Tom1 subcellular localization (Figure 18B; Katoh et al., 2004; Katoh et al, 2006). Furthermore this subcellular localization agrees with our observations both when Tom1 is overexpressed in cells of the developing chick spinal cord and

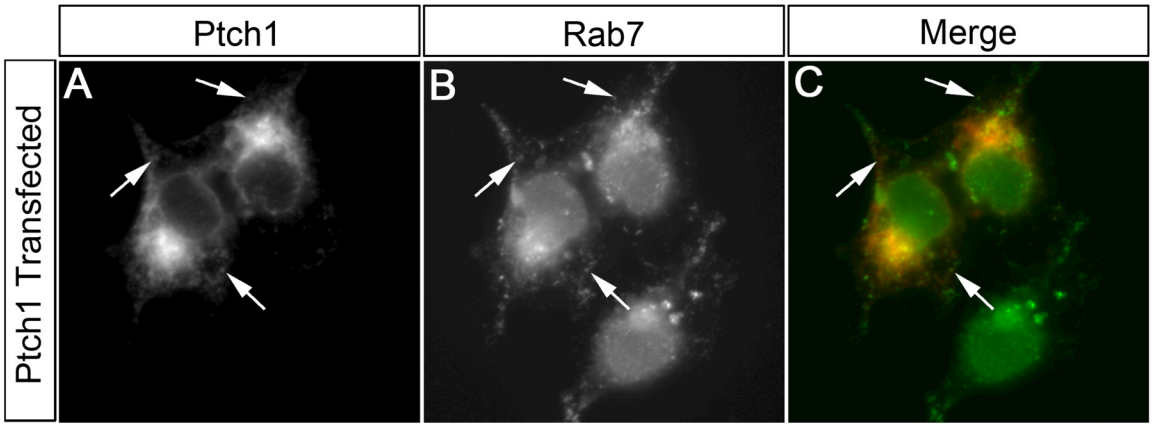

FIGURE 17. Ptch1 was detected in late endosomes in HEK293 cells. (A-C) Ptch1 transfected cells immunostained for Ptch1 (A), late endocytic marker Rab7 (B), and merged image (C). Arrows points to co-localized punctae.

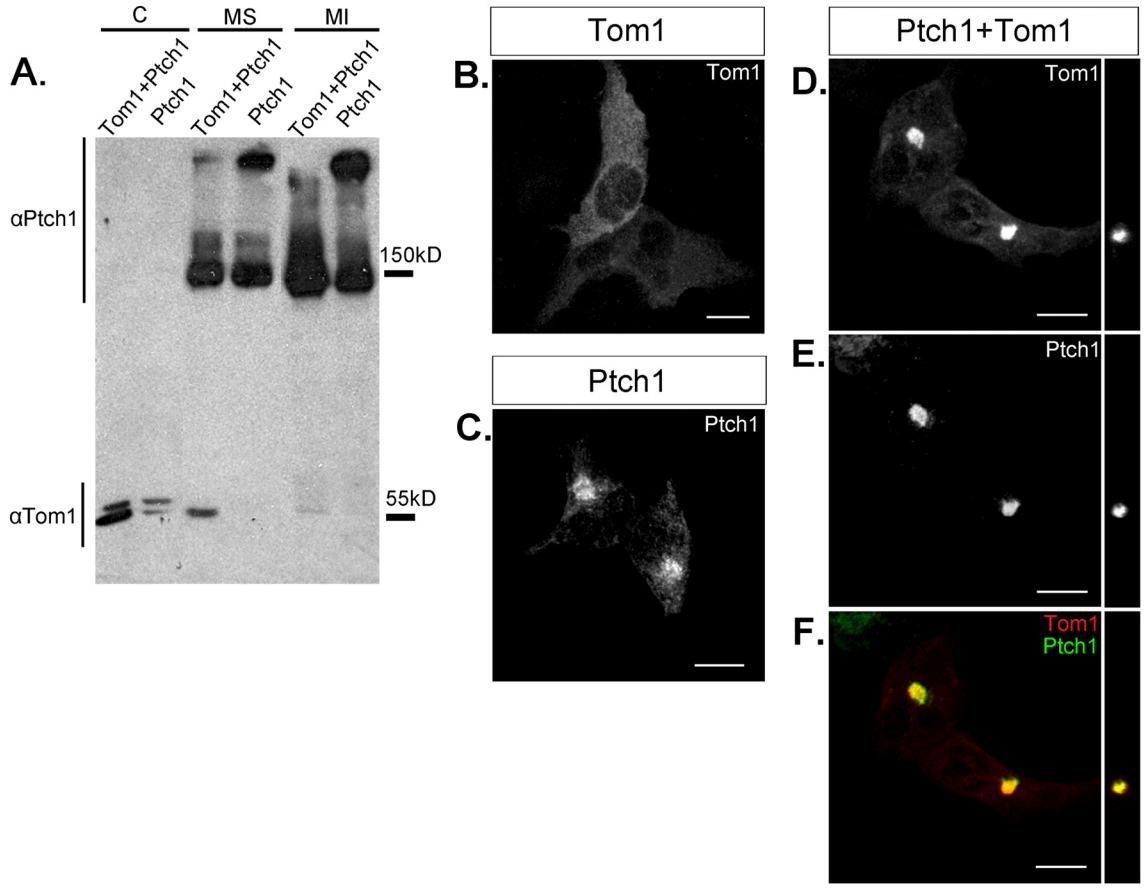

FIGURE 18. Tom1 overexpression promoted the formation of Ptch1 cytoplasmic aggregates in HEK293 cells. (A) Ptch1 and Tom1 immunoblot of lysates from a subcellular fractionation of HEK293 cells. Ptch1 localized to the membrane soluble and membrane insoluble fraction, while Tom1 localized to the cytoplasmic and membrane soluble fractions. (B) Tom1 immunostaining throughout the cytoplasm in HEK293 cells following Tom1 transfection. (C) Ptch1 immunostaining following Ptch1 transfection in HEK293 cells. Ptch1 staining concentrated around the perinuclear region, but was widely distributed throughout the cell. (D-F) Tom1 (D), Ptch1 (E) immunostaining following their co-transfection in HEK293 cells. (F) Merged image showed that both Tom1 (red) and Ptch1 (green) strongly co-localized to a single aggregate. Ptch1 exclusively localized to the aggregate following co-transfection with Tom1. Scale bar 10μm.

endogenous Tom1 expression in the developing neural tube and cerebellum (Figures 13&14).

When Tom1 and Ptch1 were overexpressed in the same cell, they showed a distinctly different localization. Tom1 remained weakly dispersed throughout the cytoplasm but also became highly localized to a circular aggregate in the perinuclear region (Figure 18 D-F). When overexpressed with Tom1, Ptch1 became strongly restricted to this aggregate. Aggregates were also found in cells overexpressing only Ptch1, but significantly more aggregates were found in cells that expressed both Tom1 and Ptch1: 17% of cells transfected with Ptch1 vs. 49% of cells transfected with both Ptch1 and Tom1 (Students t test $p < 0.001$; Figure 19). No aggregates were found in cells expressing Tom1 alone. Aggregates containing Ptch1 and Tom1 were not nonspecific protein aggregates because co-transfected EGFP did not localize to them (Figure 19 B-D). Overexpressed Ptch1 has previously been shown to induce apoptosis (Thibert et al., 2003). Therefore we assessed transfected cells for the apopototic marker cleaved caspase 3. Transfected cells did not stain positively for cleaved caspase 3 (Figure 20).

To determine the identity of these aggregates the cells were stained using an antibody specific for both mono- and poly ubiquitinated proteins (Table 3). Ptch1 and Tom1 positive aggregates stained positively for ubiquitinated proteins (Figure 21A-C). Aggregates that formed when Ptch1 was transfected alone also stained positively for ubiquitinated proteins but not as strongly (Figure 21D-F). This indicated that Tom1 may promote the localization of ubiquitinated Ptch1 to a large perinuclear structure in the cytoplasm.

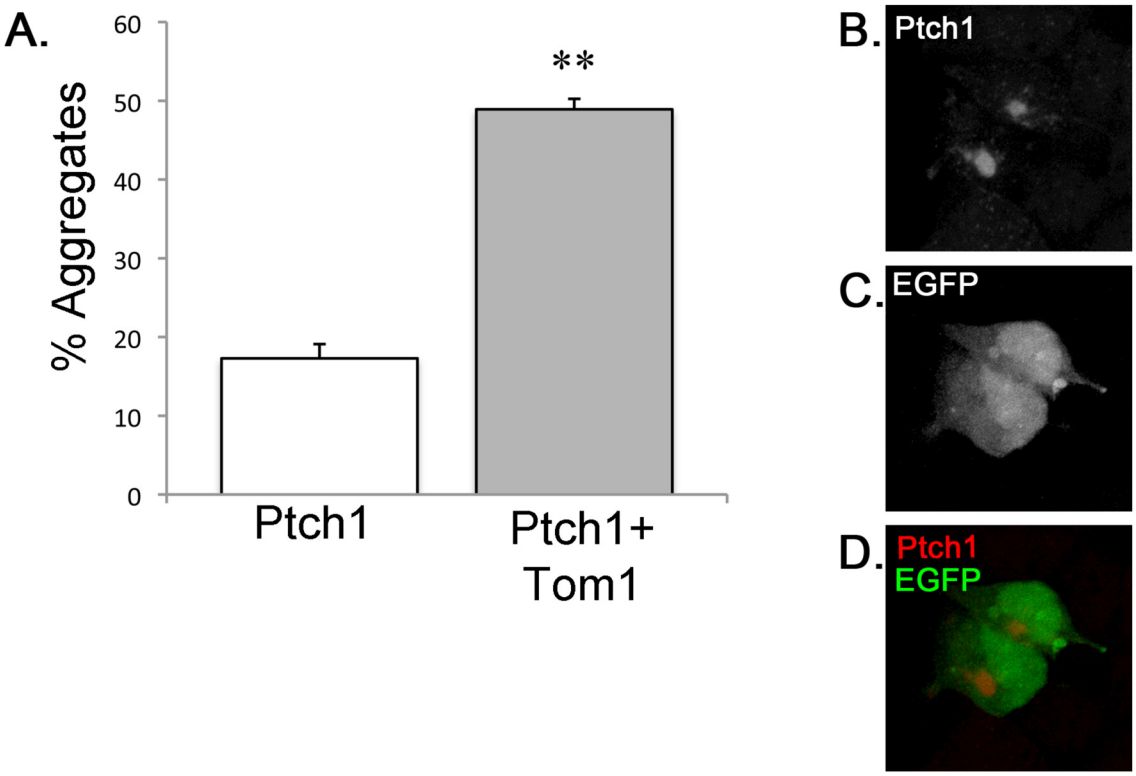

FIGURE 19. Quantification of aggregate formation in Ptch1 and Tom1 co-transfected HEK293 cells. (A) Aggregates formed in 17% (SD 3.13) of cells transfected with Ptch1 alone. Ptch1 and Tom1 co-transfection promoted Ptch1-positive aggregate formation in 49% (SD 2.31) of cells of (n=3, 100 cells counted per sample). **, P<0.001, student's t-test. (B-D) Ptch1 positive aggregates in cells expressing Ptch1 and Tom1 do not contain EGFP in control experiments. Aggregates in cells stained for Ptch1 (B), EGFP localization (C) and merged image (D).

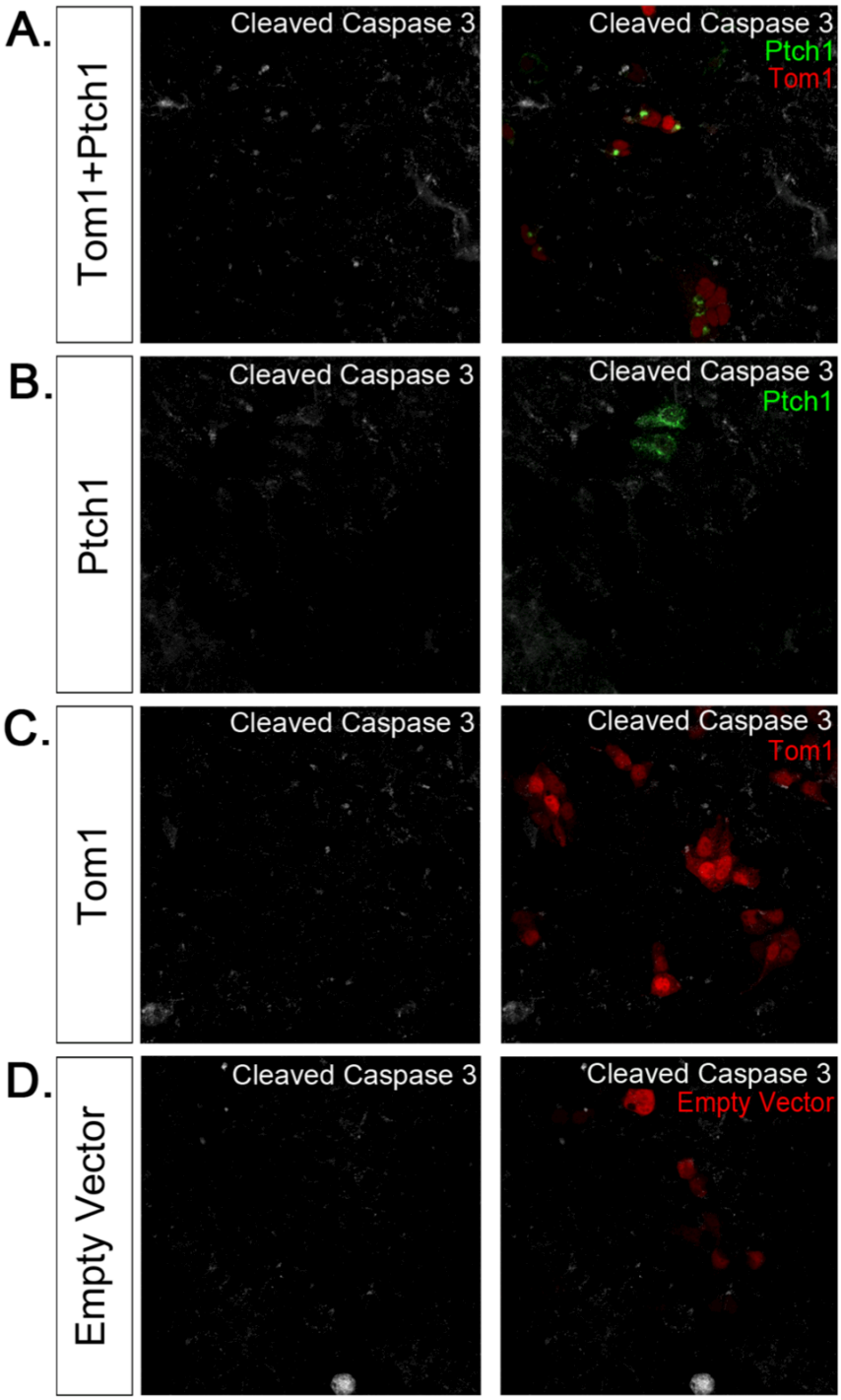

FIGURE 20. Ptch1 and Tom1 transfected cells do not stain positively for cleaved caspase 3. Cleaved caspase 3 immunostaining in HEK293 cells transfected with Tom1 and Ptch1 (A; Ptch1 immunostaining, green; Tom1 transfected cells, red), Ptch1 alone (B; Ptch1 immunostaining, green), Tom1 alone (C; Tom1 transfected cells, red), and empty vector (D; Transfected cells, red). No transfected cells stain positively for cleaved caspase 3.

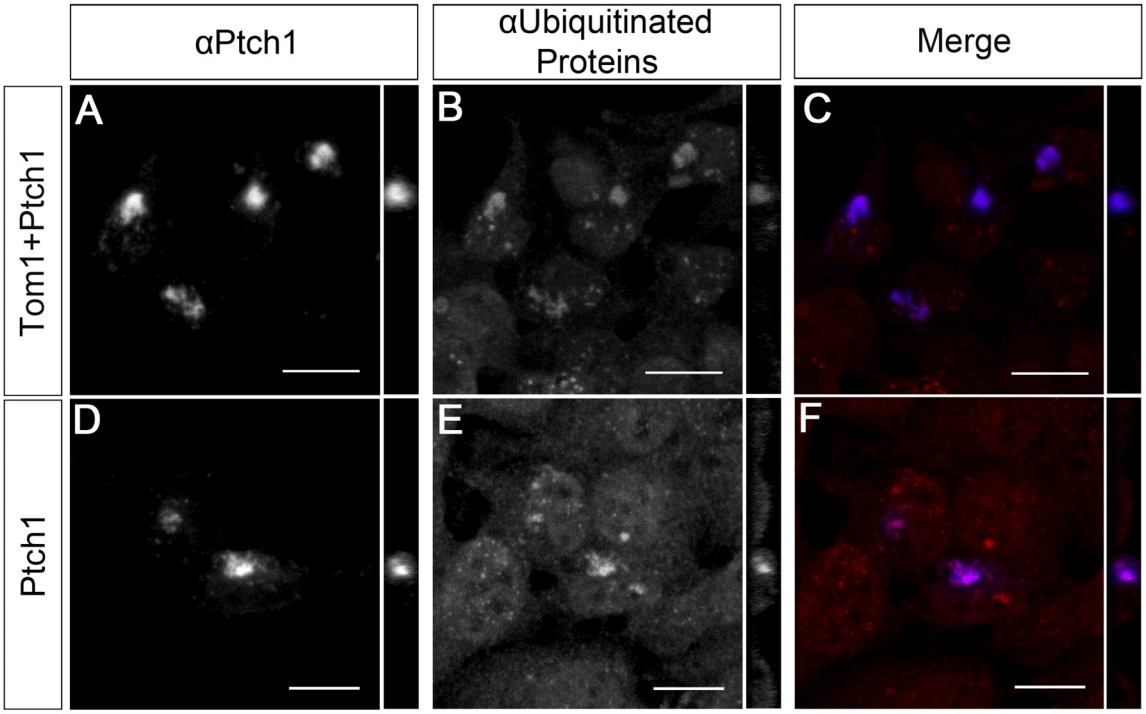

FIGURE 21. Ptch1-positive aggregates co-localized with ubiquitinated proteins. (A-C) Immunostaining of Ptch1 (A), ubiquitinated proteins (FK2 antibody, B), and merged signal (C). Ptch1 and Tom1 co-transfected HEK293 cells form aggregates that co-localized strongly with FK2 a marker for ubiquitinated proteins. (D-F) Ptch1 alone transfected cells stained for Ptch1 (D), ubiquitinated proteins (FK2, E), and merge (F), showing Ptch1-positive punctate occasional co-localized with ubiquitinated proteins. Scale bar 10μm.

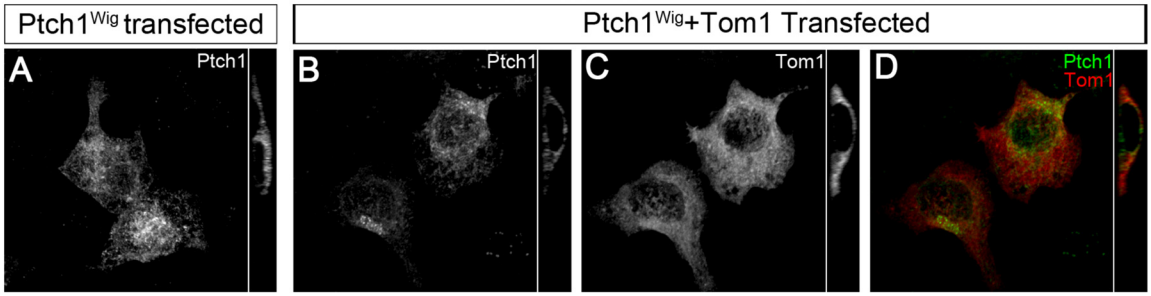

FIGURE 22. Ptch1^{Wig} did not form aggregates when co-expressed with Tom1. (A) Ptch1 immunostaining following Ptch1^{Wig} alone transfection in HEK293 cells. (B-D) Immunostaining in Ptch1^{Wig} and Tom1 co-transfected HEK293 cells for Ptch1 (B), Tom1 (C), and merge (D). Ptch1^{Wig} and Tom1 co-localized weakly when overexpressed and did not form aggregates.

When Ptch1^{Wig} was expressed alone it appeared to localize throughout the cell in punctate structures and at the plasma membrane (Figure 22A). Interestingly, when *Ptch1^{Wig}* and *Tom1* were overexpressed together they co-localized only minimally and did not form aggregates (Figure 22B-D). Furthermore, Ptch1^{Wig} co-expressed with Tom1 appeared to associate more closely with the perinuclear region, but this finding needs to be reproduced (Figure 22B). One clear difference between wild-type and Ptch1^{Wig} localization following Tom1 overexpression is that Ptch1^{Wig} failed to form a single highly concentrated perinuclear aggregate, and much staining remained scattered throughout the cytoplasm. Altogether the findings described here implicate a non-essential role for Tom1 is regulating Ptch1 cytoplasmic localization, but also revealed that Tom1 is not critically required to regulate Ptch1 function in Shh signaling in the spinal cord.

CHAPTER 4: DISCUSSION

Summary

The hedgehog pathway plays important roles in vertebrate development and tumorigenesis. A key regulator of sonic hedgehog (Shh) signaling is the transmembrane receptor Patched1 (Ptch1). While Ptch1 plays a crucial role in regulating the extent of Shh signaling in developing tissues, it is not yet clear how this receptor is turned over in the cell. The purpose of this thesis was to identify novel regulators of Ptch1. To this end, these results revealed that target of myb1 (Tom1) may be a novel regulator of Ptch1 endocytic cycling. It was shown that Tom1 interacted with the N-terminal portion of the Ptch1 (called Patched1 Wiggable; $Ptch1^{Wig}$) and was expressed in the developing mouse embryo and the adult mouse cerebellum. In addition, Tom1 was shown to have a cytoplasmic localization when detected endogenously and when overexpressed. Interestingly, when Tom1 was co-expressed with Ptch1 in human embryonic kidney (HEK293) cells, both proteins localized to large aggregates in the perinuclear region. However when Tom1 and $Ptch1^{Wig}$ were co-expressed, $Ptch1^{Wig}$ did not form aggregates. Furthermore, these results suggested that Tom1 did not have a functional role in Shh signaling during neural development, as the overexpression of Tom1 in the developing chick neural tube did not have an effect on dorso-ventral patterning of progenitor domain populations. However, given that Tom1 was also expressed in Shh target tissues in the adult brain, it is possible that it does play a role in the regulation of Ptch1 function there.

Tom1 Interacts with Ptch1^{Wig} but not Wild-type Ptch1

To validate a role for Tom1 in controlling Ptch1 endocytic cycling or degradation, the association of these two proteins was investigated using immunoprecipitation experiments in HEK293 cells. Interestingly, while Tom1 did not interact with the wild-type Ptch1 protein it did interact with a C-terminal truncated form of Ptch1 called Ptch1^{Wig}. This result was surprising as the immunofluorescence data show that Ptch1^{Wig} and Tom1 only co-localize occasionally while wild-type Ptch1 and Tom1 co-localize in perinuclear aggregates.

There are several reasons why Tom1 might not have been detected in immunoprecipitated lysates even if they do in fact bind. First, Ptch1^{Wig} is approximately 90kD and has 7 transmembrane domains while wild-type Ptch1 is approximately 150kD and has 12 membrane spanning domains. Therefore, Ptch1^{Wig} protein is more readily solubilized during protein extraction. The conditions used to extract wild-type Ptch1 from the membrane may not have allowed for the maintenance of the Ptch1-Tom1 interaction. Furthermore the co-immunoprecipitation of Ptch1^{Wig} was conducted using stable cell lines expressing *Ptch1^{Wig}* while the co-immunoprecipitation of wild-type Ptch1 was conducted using transient overexpression. Stable cell lines expressing lower levels of *Ptch1^{Wig}* may have allowed for the maintenance of the Tom1- Ptch1 interaction.

Interestingly, previous research suggests the C-terminal portion of Ptch1 regulates its turnover (Lu et al., 2006; Kawamura, 2008). Since Ptch1^{Wig} is missing the C-terminal portion of the Ptch1 protein, it is likely that Ptch1^{Wig} has a longer half-life than wild-type Ptch1. Anecdotally, Ptch1^{Wig} appeared to be present more at the cell surface than wild-

type Ptch1, which concentrates around the perinuclear region. If Tom1 interacts with Ptch1 at the cell surface or at early endosomes, $Ptch1^{Wig}$ may encounter Tom1 more often allowing for detection by co-immunoprecipitation. In order to test this possibility, co-immunoprecipitation with wild-type Ptch1 could be conducted after inhibiting early endosome maturation to late endosome using the vacuolar ATPase inhibitor concanamycin A (Incardona et al., 2000, 2002). An alternative possibility is the association of Ptch1 with Tom1 causes ubiquitination and destruction of the complex. Therefore detection of the interaction would not be possible. In order to test this, the co-immunoprecipitations experiments could be repeated using the proteosome inhibitor MG132.

Expression of Tom1 in Embryo and Adult Cerebellum

To my knowledge this study is the first to investigate the expression of Tom1 in the developing mouse and chick embryo. Using RT-PCR and Western blot it was shown that *Tom1* is expressed at E10.5 in the mouse embryo and at E3.5 in the chick embryo. At these stages in the chick and mouse embryo Shh signaling is patterning the nervous system and Ptch1 is highly expressed (Matise and Wang, 2011). *Tom1* mRNA in all embryo stages studied appeared to be low and ubiquitous expression with no apparent increased labeling of distinct structures. Tom1 protein expression was also low, and enhancement of the signal was necessary to detect its expression. Interestingly, Tom1 protein was expressed in the E9.5 neural tube and appeared to have higher levels dorsally than ventrally. This pattern was the inverse of the Ptch1 expression pattern. It is

interesting to speculate that Tom1 could be involved in negatively regulating Ptch1 protein levels throughout the neural tube during patterning.

In contrast to Tom1 expression in the embryo, high throughput expression screens have suggested that Tom1 has a tissue specific expression pattern in the adult. Using antibody-based proteomics, the Human Protein Atlas (www.proteinatlas.org) found that Tom1 is expressed in molecular layer interneurons and Purkinje cells, and is absent from the granular cell layer of the human adult cerebellum. These results confirmed that the adult mouse cerebellum also expresses Tom1 in the molecular layer and in Purkinje cells.

In addition to the role of Shh in patterning the embryo, Shh and downstream components, including Ptch1, continue to be expressed in the adult. Recently Petralia et al. (2011 and 2012) examined the subcellular distribution of Ptch1 and Smo in the adult cerebellum and hippocampus. Interestingly they found that Ptch1 and Smo are localized to dendritic spines, endosomes and autophagosomes. Tom1 localizes to endosomes through its interaction with Endofin and Tollip. Interestingly, Tom1 was recently shown to be involved in the delivery of endosomes to autophagosomes and their subsequent fusion with the lysosome (Tumbarello et al., 2012). These observations suggest that Tom1 may play a role in shuttling Ptch1 in various subcellular compartments such as endosomes and autophagosomes.

During development, Shh diffusing from the Purkinje cells induces the proliferation of granular neuronal precursors and differentiation of Bergmann Glia (Dahmane and Altaba, 1999). However, the role of Shh in the adult cerebellum is unknown. It is possible that Tom1 in the adult cerebellum may regulate an alternative

endocytic cycling pathway for Ptch1. However this is speculative and more research will have to be done to investigate this possibility.

Tom1 Does Not Have a Functional Role in Dorso-ventral Patterning of the Neural Tube

The role for Tom1 in Ptch1-mediated Shh signaling is not known. However, the cellular and biochemical analyses indicated that Tom1 may play a role in subcellular localization of Ptch1. Therefore, Tom1 function in Shh signaling was analyzed in the context of neural tube patterning, which is highly influenced by Shh. The hypothesis addressed was, if Tom1 plays a role in Ptch1 endocytosis and ultimately destruction, then its overexpression should result in the expansion of ventral progenitor identity in the developing spinal cord.

The results indicated that Tom1 overexpression does not alter Shh signaling in the developing neural tube. Electroporation of Tom1 or EGFP caused shifts in Nkx2.2, Olig2 and Pax6 progenitor domains. These shifts were qualitatively similar in both conditions, and only amounted to one or two cell layers, or a few ectopic cells. It is unclear why this effect was observed only on the electroporated side in both experimental and control conditions. However, GFP, and the bacterial protein lipopolysaccharide (LPS) have both previously been reported to be cytotoxic (Lui et al., 1999; Cotton et al., 1994). LPS is a major component of the gram-negative bacterial cell wall, in which the plasmid DNA was amplified and is a common contaminant of plasmid DNA preparations (Cotton et al., 1994). Given that both experimental and control vectors used for electroporation also expressed GFP, and were prepared under the same conditions, one possibility is that electroporation of plasmid DNA was slightly toxic to cells under the

conditions used. Indeed anecdotally it was observed that the electroporated side is sometimes smaller than the unelectroporated side. As Shh is a diffusible protein, fewer cells might allow the protein to diffuse further causing induction of downstream target genes more dorsal that normal, producing the observed effects on patterning.

There are several reasons why there might not be an effect on Shh patterning in response to Tom1 overexpression. First it was shown that Tom1 is already expressed in the developing neural tube. Tom1 may be required for proper Ptch1 endocytic cycling, but expressing excess Tom1 may not cause this process to occur more efficiently and therefore have no effect on target gene activation. Another possibility is Tom1 may be altering Ptch1 endocytic cycling after Shh has already induced the activation of target genes. In *Drosophila*, blocking dynamin-mediated endocytosis of Ptch1 does not affect Shh target gene activation suggesting endocytosis is not required for normal Shh signaling (Torroja et al., 2004). If Tom1 were acting downstream of endocytosis and facilitating Ptch1 degradation, Shh signal transduction may have already been relayed to the cell and patterning would not be affected.

However in contrast to studies in *Drosophila*, using chick embryo explants Incardona et al., (2002) found that disrupting the late endosome also disrupted downstream Shh signaling. This suggested that endosomal sorting, at least in vertebrate cells, is required for proper Shh signaling. Furthermore, Rohaghi et al., (2007) suggested that Ptch1 is normally present at the primary cilium and removal of Ptch1 from the primary cilium allows for a concomitant increase of Smo required for pathway activation. Together this evidence suggests that endocytic regulation of Ptch1 and the Ptch1-Shh complex is critical to the regulation of downstream signaling.

Yet another explanation for why there was no observed effect of Tom1 overexpression is the deficiency of another protein required for Tom1 function. Tom1 interacts and is targeted to the endosome by both Tollip and Endofin. Indeed overexpression of Tom1 has a cytoplasmic localization, while overexpressing both Tom1 with Tollip or Endofin causes a punctate endosomal pattern of expression (Katoh et al., 2004; Seet et al., 2004). Localization of Tom1 to the endosome may be necessary for its functional regulation of Ptch1. Therefore Tom1 overexpression alone may not be sufficient to perturb signaling.

Non-canonical Hedgehog Signaling

In addition to the role of Shh in patterning, several non-canonical signaling pathway's initiated by Ptch1 have been found (Jenkins, 2009). Ptch1 is thought to act as a dependence receptor promoting apoptosis in the absence of Shh (Thibert et al., 2003; Fombone et al., 2012). Furthermore unbound Ptch1 has been shown to bind cyclin B1 preventing its translocation to the nucleus and promotion of cell cycle progression (Barnes et al., 2001). Endocytic cycling of cell surface receptors has recently been implicated in having diverse effects on how the cell receives and interprets extracellular signals (Platta and Stenmark, 2011). Indeed it has been shown that the duration the cell receives the signal as well as the subcellular localization of endocytosed receptors can have diverse effects on downstream signaling (Nowak et al., 2011). It is possible that endocytic regulation by Tom1 could be affecting another function of Ptch1 or Shh apart from canonical Smo and Gli mediated signal transduction. This would not have been detected by assessing dorso-ventral patterning of the spinal cord. However, more research

assessing the other functions of Ptch1 including apoptosis and cell cycle progression are needed to assess this possibility.

Tom1 and Ptch1 Co-localize in Perinuclear Aggregates

To examine the subcellular relationship between Tom1 and Ptch1, proteins were overexpressed in HEK293 cells. Overexpression of Tom1 and Ptch1 together caused their accumulation in large aggregates in the perinuclear region. In the absence of Tom1, Ptch1 also localized to similar structures but less strongly and frequently, while Tom1 never showed this pattern in the absence of Ptch1. Importantly, the protein aggregate stains positively for ubiquitinated proteins. To my knowledge this is the first time in mammalian cells that Ptch1 has been shown to co-localize with markers for ubiquitinated proteins, and this is the first time Tom1 has been shown to localize in large protein aggregates. This supports the hypothesis that Ptch1 is ubiquitinated as part of its turnover and suggests that Tom1 may play a role in aggregate formation and/or clearance from the cell.

Ptch1 is thought to be ubiquitinated because the C-terminus of Ptch1 co-immunoprecipitates with the E3 ubiquitin ligases Smurf2 and Nedd4 (Lu et al., 2006). E3 ubiquitin ligases catalyse the third and final step of ubiquitination resulting in the attachment of ubiquitin to a lysine residue. Furthermore Ptch1 ubiquitination is thought to target it to the lysosome for degradation (Gallet and Therond 2005; Incardona et al., 2000; Torroja et al., 2004). Thus, Ptch1 ubiquitination has important consequences for Ptch1 turnover and competence to respond to Shh signaling. Several lines of evidence suggest that Tom1 is involved in the process degradation of ubiquitinated proteins from

the endosomal pathway. First, Tom1 is known to interact with ubiquitinated proteins through its GAT and possibly VHS domain (Shiba, 2003; Akutsu et al., 2005). Also, along with Tollip, Tom1 is capable of recruiting ubiquitinated proteins to the early endosome (Katoh et al., 2004). Furthermore, knockdown of Tom1 in HeLa cells causes the accumulation of endosomes containing ubiquitinated proteins (Tumbarello et al., 2012).

Interestingly, knocking down the ESCRT-0 protein Hrs in *Drosophila* imaginal wing disc caused the accumulation of Ptch1 in large endosomes that also stained positively for ubiquitinated protein. Hrs and Tom1 are thought to share a similar function as they both contain a VHS domain, bind ubiquitinated proteins and clathrin, and are targeted to the endosomal membrane (Jekely and Rorth, 2003; Wang et al., 2010). Given that Tom1 binds ubiquitinated proteins, Ptch1 is ubiquitinated and that both proteins co-localize in aggregates of ubiquitinated proteins it is likely that Tom1 binds to ubiquitinated Ptch1.

When Ptch1 and Tom1 are expressed together the structure that forms resembles an aggresome. Aggresomes are juxtanuclear inclusion bodies (protein aggregates) that can form in response to proteosome inhibition, cell stress or overexpression of certain proteins (Johnsten et al., 1998). Aggresomes are thought to form as the result of the accumulation of misfolded proteins that overwhelm both the chaperones that correct misfolding and cellular degradation machinery (Johnston et al., 1998; Corbey et al., 2005). They localize to the centrosome and stain positively for ubiquitinated proteins (Corbey et al., 2005). Aggresomes are then subsequently removed from the cell by autophagy. It is likely that aggregates containing Tom1 and Ptch1 that were observed are

in fact aggresomes, however, in order to verify the identity of these structures, confirmation that they localize to the centrosome is required.

There is some debate as to whether the formation of aggresomes promotes cell survival or is instead cytotoxic to the cell. One study found that aggresome formation impairs the ubiquitin-proteosome system (Bence et al., 2001). Given the importance of this system in cellular regulation of the proteome, this suggests that it would impair cell function and eventually cause cell death. However, most recent research suggests that aggresomes are protective, because they sequester potentially toxic proteins and facilitate their clearance from the cell by autophagy (Olzman et al., 2008).

Inclusion bodies are observed in many diseases including Huntington's disease, Cystic fibrosis, ALS and Alzhiemer's Disease (Olzman et al., 2008). Aggresome formation is largely an artifact of cell culture, but studying it provides important insights into how protein aggregates are formed and cleared from the cell. Interestingly autophagic machinery, including the protein microtuble associated protein light chain 3 (LC3), which is widely used as an autophagosome marker, accumulates at the aggresome as well (Jänen et al., 2010).

A recent report also showed for the first time that Tom1 plays an important role in autophagic degradation from the endocytic pathway. Tumberello et al. (2012) showed that Tom1 interacts with myosin VI through it C-terminus (final 104 aa). Myosin VI is a retrograde actin motor protein important for endocytic vesicle delivery to autophagosomes, and autophagosome subsequent fusion with the lysosome. Tom1 was found to be required for targeting of myosin VI to Rab5 positive vesicles (a marker for early endosomes) as loss of Tom1 resulted in loss of myosin VI and Rab5 co-localization

(Tumberello eta al., 2012). Strikingly, loss of Tom1 also causes the accumulation of LC3 positive autophagosomes and accumulation of ubiquitin positive punctate. This is similar to what was observed when Hrs was knocked out in the *Drsosophila* wing imaginal disc. However, knocking down myosin VI prevented fusion of endocytic vesicles with autophagosome (Tumberello et al., 2012). If Tom1 overexpression were facilitating Ptch1 localization from the endocytic pathway to the autophagosome, the protein aggregation that I observed may reflect the limited capacity of the cell to degrade the large amount of protein directed through this pathway. Cellular machinery such as myosin VI may be limited and therefore efficient degradation of protein may not be possible causing aggregates to form.

Alternatively, overexpressed Ptch1 may overwhelm the protein synthesis apparatus causing it to be misfolded, and preventing it from being properly inserted into the membrane. Tom1 may be therefore be involved in aggresome formation sequestering and transporting insoluble Ptch1 aggregates to the microtubule organizing centre for more efficient degradation. To test whether or not Ptch1 aggregates are composed of protein delivered from the cell surface, fluorescently labeled dextran could be used to label the endocytic pathway in Tom1 and Ptch1 co-transfected cells (Incardona, 2000). Co-localization between the dextran and Ptch1 would indicate it was transported from the cell surface.

Although most reports of Tom1 subcellular localization suggest that Tom1 localizes to the cytoplasm and endosomes, the human protein atlas found that Tom1 associates with the centrosome in the cell line A431 (http://www.proteinatlas.org/ENSG00000100284/subcellular). This staining appears

similar to Tom1 localization when overexpressed with Ptch1. A431 is a squamous carcinoma cell line known to express abnormally high levels of the epidermal growth factor receptor (EGFR). Tom1 interacts with endofin, which is phosphorylated in response to EGF signaling and co-localizes with EGFR on endosomes (Seet et al., 2004; Toy et al., 2010). However, Tom1 has not been shown to be involved in EGF signaling but this suggests localization to the centrosome is a characteristic of Tom1 function.

Tom1 protein expression is also regulated by the microRNA miR-126 (Oglesby et al., 2010). MiR-126 was recently reported to be downregulated in cystic fibrosis airway epithelial cells while Tom1 protein showed a concomitant upregulation (Oglesby et al., 2010). Tom1 overexpression prevents the activation of the proinflammatory transcription factor NF-κB, by IL1β, TNFα and LPS (Oglesby et al., 2010; Yamanaki and Yokosawa, 2004). This suggests that Tom1 has a negative role in the inflammatory response. Upregulation of Tom1 in cystic fibrosis epithelial cells may therefore reflect a compensatory mechanism in response to the excess inflammation that occurs in cystic fibrosis. Interestingly Tom1 protein is also upregulated (presumably through miR-126 downregulation) in response to ER stress (Oglesby et al., 2010). In cystic fibrosis, aggregates containing cystic fibrosis transmembrane conductance receptor (CFTR) are found in patients' airway epithelial cells but it is unclear if Tom1 upregulation plays a role in this or is activated as a compensatory mechanism (Luciani et al. 2010).

Unexpectedly, transfecting Tom1 with Ptch1^{Wig} does not cause Ptch1^{Wig} to form aggregates. This suggests the C-terminal portion of Ptch1 may mediate this effect. Given that the C-terminus is known to regulate Ptch1 turnover this may suggest Ptch1

aggregates form from Ptch1 traveling through a degradative pathway (Lu et al., 2006; Kawamura et al., 2008).

In contrast, Ptch1^{Wig} because of its smaller size (90kD vs 150kD) and the absence of the C-terminus, would be less prone to both degradation and aggregation. This begs the question of why an interaction between Ptch1^{Wig} and Tom1 using co-immunoprecipitation of Ptch1^{Wig} stable cell lines was found, but Tom1 and Ptch1^{Wig} did not co-localize when transfected together. However, in the Ptch1^{Wig} stable cell lines the wild-type *Ptch1* locus is intact. Given that Ptch1^{Wig} acts as a Shh gain of function, and *Ptch1* is a transcriptional target of Shh, Ptch1^{Wig} expression would cause the upregulation of wild-type *Ptch1*. Ptch1 is thought to exist as a homotrimer (Lu et al., 2006), and in *Drosophila*, C-terminal truncations of Ptch1 are able to associate with wild-type Ptch1 (Lu et al., 2006). Therefore Ptch1^{Wig} is likely forming heterotrimers with wild-type Ptch1 and this could mediate the interaction with Tom1. However in transient transfected cell lines, the amount of *Ptch1*^{Wig} expression likely overwhelmed wild-type *Ptch1* upregulation, explaining why only minimal co-localization between Tom1 and Ptch1^{Wig} was detected.

Together my results suggest that Tom1 may be a regulator of Ptch1 endocytic cycling. Under my experimental conditions, Ptch1 is an aggregate prone protein. However, to my knowledge, Ptch1 has not been found to cause aggregates in cell culture or co-localize with markers for ubiquitinated proteins in vertebrates before. Furthermore, it was shown for the first time that Tom1 promoted the formation of Ptch1 aggregates. This is a significant finding since recent research has separately implicated a role for Tom1 in autophagy, as well as demonstrating Ptch1 localizes to the autophagosome

(Petrolia et al., 2011, 2012). It is interesting to speculate that endocytosed Ptch1 destined for degradation may not be transported directly to the lysosome, but may first fuse with the autophagosome. Overexpression of Tom1 may precipitate a degradation route for intracellular Ptch1, and this process most certainly requires a complex biochemical machinery to efficiently target Ptch1 to the autophagosome. Therefore, Tom1 could be a novel candidate involved in aggresome formation that can promote the targeting of Ptch1 to the autophagosome. Given that Tom1 is upregulated in cysitic fibrosis leading to the formation of aggregates of the CFTR (Luciani et al., 2010), future studies should examine if Tom1 is also upregulated in diseases involving the aberrant formation of protein aggregates.

Conclusions

Understanding the endocytic cycling and degradation pathway of Ptch1 has important implications for how cells respond to levels of Shh signaling, in both normal and diseased tissues. This thesis has explored the role of Ptch1 endocytic cycling and aggresome formation, and has implicated the novel adapter protein Tom1 in this process. This work will lead to further studies that will determine how Tom1 affects Ptch1 steady state levels in live cells, and whether it is a contributing factor in tumors induced by aberrant Shh signaling.

REFERENCES

Akutsu, M., Kawasaki, M., Katoh, Y., Shiba, T., Yamaguchi, Y., Kato, R., Kato, K., Nakayama, K. & Wakatsuki, S. Structural basis for recognition of ubiquitinated cargo by Tom1-GAT domain. FEBS Letters 579, 5385-5391 (2005).

Barnes, E.A., Kong, M., Ollendorff, V. & Donoghue, D.J. Patched1 interacts with cyclin B1 to regulate cell cycle progression. EMBO J 20, 2214-2223 (2001).

Beachy, P.A., Hymowitz, S.G., Lazarus, R.A., Leahy, D.J. & Siebold, C. Interactions between Hedgehog proteins and their binding partners come into view. Genes Dev 24, 2001-2012 (2010).

Bidet, M., Joubert, O., Lacombe, B., Cianter, M., Nehme, R., Mollat, P., Bretillon, L., Faure, H., Bittman, R., Ruat, M. & Mus-Veteau, I. The hedgehog receptor patched is involved in cholesterol transport. PLoS ONE 6, e23834 (2011).

Blanc, C., Charette, S., Mattei, S., Abrey, L., Smith, E., Cosson, P. & Letourneur, F. Dictyostelium Tom1 participates to an ancestral ESCRT-0 complex. Traffic 10, 161-171 (2009).

Briscoe, J. & Novitch, B.G. Regulatory pathways linking progenitor patterning, cell fates and neurogenesis in the ventral neural tube. Philosophical Transactions of the Royal Society B: Biological Sciences 363, 57-70 (2008).

Briscoe, J., Chen, Y., Jessell, T.M. & Struhl, G. A hedgehog-insensitive form of patched provides evidence for direct long-range morphogen activity of sonic hedgehog in the neural tube. Mol. Cell 7, 1279-1291 (2001).

Briscoe, J., Sussel, L., Serup, P., Hartigan-O'Connor, D., Jessell, T., Rubenstein, J. & Ericson, J. Homeobox gene Nkx2.2 and specification of neuronal identity by graded Sonic hedgehog signalling. Nature 398, 622-627 (1999).

Brissoni, B., Agostini, L., Kropf, M., Martinon, F., Swoboda, V., Lippens, S., Everett, H., Aebi, N., Janssens, S., Meylan, E., Felberbaum-Corti, M., Hirling, H., Gruenber, J., Tschopp, J. & Burns, K. Intracellular trafficking of interleukin-1 receptor I requires Tollip. Curr Biol 16, 2265-2270 (2006).

Buglino, J.A. & Resh, M.D. Palmitoylation of Hedgehog Proteins. Hedgehog Signaling 88, 229-252 (Elsevier Inc.: 2012).

Burk, O., Worpenberg, S., Haenig, B. & Klempnauer, K.H. tom-1, a novel v-Myb target gene expressed in AMV- and E26-transformed myelomonocytic cells. EMBO J 16, 1371-1380 (1997).

Callejo, A., Culi, J. & Guerrero, I. Patched, the receptor of Hedgehog, is a lipoprotein receptor. PNAS, 105, 912-917 (2008).

Capdevila, J., Pariente, F., Sampedro, J., Alonso, J.L. & Guerrero, I. Subcellular localization of the segment polarity protein patched suggests an interaction with the wingless reception complex in Drosophila embryos. Development 120, 987-998 (1994).

Casali, A. & Struhl, G. Reading the Hedgehog morphogen gradient by measuring the ratio of bound to unbound Patched protein. Nature 431, 76-80 (2004).

Caspary, T., García-García, M., Huangfu, D., Eggenschwiler, J., Wyler, M., Rakeman, A., Alcorn, H., & Anderson, K. Mouse Dispatched homolog1 is required for long-range, but not juxtacrine, Hh signaling. Curr Biol 12, 1628-1632 (2002).

Corbit, K.C., Aanstad, P., Singla, W., Norman, A., Stainier, D. & Reiter, J. Vertebrate Smoothened functions at the primary cilium. Nature 437, 1018-1021 (2005).

Corboy, M.J., Thomas, P.J. & Wigley, W.C. Aggresome formation. Methods Mol. Biol. 301, 305-327 (2005).

Dahmane, N. & Ruiz i Altaba, A. Sonic hedgehog regulates the growth and patterning of the cerebellum. Development 126, 3089-3100 (1999).

Denef, N., Neubüser, D., Perez, L. & Cohen, S.M. Hedgehog induces opposite changes in turnover and subcellular localization of patched and smoothened. Cell 102, 521-531 (2000).

Dennis, J.F., Kurosaka, H., Iulianella, A., Pace, J., Thomas, N., Beckham, S., Williams, T. & Trainor, P. Mutations in hedgehog acyltransferase (hhat) perturb hedgehog signaling, resulting in severe acrania-holoprosencephaly-agnathia craniofacial defects. PLoS Genet. 8, e1002927 (2012).

Dessaud, E., McMahon, A.P. & Briscoe, J. Pattern formation in the vertebrate neural tube: a sonic hedgehog morphogen-regulated transcriptional network. Development 135, 2489-2503 (2008).

Dessaud, E., Yang, L., Hill, K., Cox, B., Ulloa, F., Ribeiro, A., Mynett, A., Novitch, B. & Briscoe, J. Interpretation of the sonic hedgehog morphogen gradient by a temporal adaptation mechanism. Nature 450, 717-720 (2007).

Ericson, J., Rashbass, P., Schedl, A., Brenner-Morton, S., Kawakami, A., Heyningen, V., Jessell, T. & Briscoe, J. Pax6 controls progenitor cell identity and neuronal fate in response to graded Shh signaling. Cell 90, 169-180 (1997).

Etheridge, L.A., Crawford, T.Q., Zhang, S. & Roelink, H. Evidence for a role of vertebrate Disp1 in long-range Shh signaling. Development 137, 133-140 (2010).

Fader, C.M. & Colombo, M.I. Autophagy and multivesicular bodies: two closely related partners. Cell Death Differ 16, 70-78 (2008).

Filimonenko, M., Stuffers, S., Raiborg, C., Yamamoto, A., Malerød, L., Fisher, E., Isaacs, A., Brech, A., Stenmark, H. & Simonsen, A. Functional multivesicular bodies are required for autophagic clearance of protein aggregates associated with neurodegenerative disease. J. Cell Biol. 179, 485-500 (2007).

Flynn, D., Adapter Proteins. Oncogene, 20, 6270-6272 (2001).

Fombonne, J., Bissey., P., Guix, C., Sadoul, R., Thibert, C. & Mehlen, P. Patched dependence receptor triggers apoptosis through ubiquitination of caspase-9. Proc Natl Acad Sci USA (2012).doi:10.1073/pnas.1200094109

Gallet, A. & Therond, P.P. Temporal modulation of the Hedgehog morphogen gradient by a patched-dependent targeting to lysosomal compartment. Dev Biol 277, 51-62 (2005).

Hochstrasser, M. Ubiquitin-Dependent Protein Degradation. Annu Rev Genet, 30, 405-439, (1996).

Incardona, J.P., Gaffield, W., Lange, Y., Cooney, A., Pentchev, P., Liu, S., Watson, J., Kapur, R. & Roelink. Cyclopamine Inhibition of Sonic Hedgehog Signal Transduction Is Not Mediated through Effects on Cholesterol Transport. Dev Biol 224, 440-452 (2000a).

Incardona, J.P., Gruenberg, J. & Roelink, H. Sonic hedgehog induces the segregation of patched and smoothened in endosomes. Curr Biol 12, 983-995 (2002).

Incardona, J.P., Lee, J., Robertson, C., Enga, K., Kapur, R. & Roelink. Receptor-mediated endocytosis of soluble and membrane-tethered Sonic hedgehog by Patched-1. Proc Natl Acad Sci USA 97, 12044-12049 (2000b).

Ingham, P.W. & Mcmahon, A.P. Hedgehog signaling in animal development: paradigms and principles. Genes Dev 15, 3059-3087 (2001).

Jänen, S.B., Chaachouay, H. & Richter-Landsberg, C. Autophagy is activated by proteasomal inhibition and involved in aggresome clearance in cultured astrocytes. Glia 58, 1766-1774 (2010).

Jékely, G. & Rørth, P. Hrs mediates downregulation of multiple signalling receptors in Drosophila. EMBO Rep 4, 1163-1168 (2003).

Jenkins, D. Hedgehog signalling: emerging evidence for non-canonical pathways. Cell Signal 21, 1023-1034 (2009).

Jeong, J. & McMahon, A.P. Growth and pattern of the mammalian neural tube are governed by partially overlapping feedback activities of the hedgehog antagonists patched 1 and Hhip1. Development 132, 143-154 (2005).

Jiang, X., Yang, P. & Ma, L. Kinase activity-independent regulation of cyclin pathway by GRK2 is essential for zebrafish early development. Proc Natl Acad Sci USA 106, 10183-10188 (2009).

Jin, Y., Chen, C., Meng, L., Chen, J., Li, M., Zhu, Z. & Lin, J. A CE-LIF method to monitor autophagy by directly detecting LC3 proteins in HeLa cells. Analyst 137, 5571-5575 (2012).

Johnston, J.A., Ward, C.L. & Kopito, R.R. Aggresomes: a cellular response to misfolded proteins. J. Cell Biol. 143, 1883-1898 (1998).

Jullien, J. & Gurdon, J. Morphogen gradient interpretation by a regulated trafficking step during ligand-receptor transduction. Genes Dev 19, 2682-2694 (2005).

Kar, S., Deb, M., Sengupta, D., Shilpi, A., Bhutia, S. & Patra, S. Intricacies of hedgehog signaling pathways: a perspective in tumorigenesis. Experimental Cell Research 318, 1959-1972 (2012).

Katoh, Y. Tollip and Tom1 Form a Complex and Recruit Ubiquitin-conjugated Proteins onto Early Endosomes. Journal of Biological Chemistry 279, 24435-24443 (2004).

Kawamura, S., Hervold, K., Ramirez-Weber, F., Kornberg, T., Two patched protein subtypes and a conserved domain of group I proteins that regulates turnover. The Journal of Biological Chemistry 283, 30964-30969 (2008)

Kenney, A.M., Cole, M.D. & Rowitch, D.H. Nmyc upregulation by sonic hedgehog signaling promotes proliferation in developing cerebellar granule neuron precursors. Development 130, 15-28 (2003).

Lallemand, D. NF2 deficiency promotes tumorigenesis and metastasis by destabilizing adherens junctions. Genes Dev 17, 1090-1100 (2003).

Lewis, P.M., Dunn, M., McMahon, J., Logan, M., Martin, J., St-Jacques, B. & McMahon, A. Cholesterol modification of sonic hedgehog is required for long-range signaling activity and effective modulation of signaling by Ptc1. Cell 105, 599-612 (2001).

Lindström, E., Shimokawa, T., Toftgård, R. & Zaphiropoulos, P.G. PTCH mutations: distribution and analyses. Hum. Mutat. 27, 215-219 (2006).

Liou, W., Geuze, H., Geelen, M., & Slot, J. The Autophagic and Endocytic Pathways Converge at the Nascent Autophagic Vacuoles. J Cell Biol 136, 61-70 (1996).

Lu, X. The C-terminal tail of the Hedgehog receptor Patched regulates both localization and turnover. Genes Dev 20, 2539-2551 (2006).

Luciani, A., Villella, V., Esposito, S., Brunetti-Pierri, N., Medina, D., Settembre, C., Gavin, M., Pulze, L., Giardino, I., Pettoello-Mantovani, M., D'Apolito, M., guido, S., Masliah, E., Spencer, B., Quaratino, S., Raia, V., Ballabio, A., & Maiuri, L. Defective CFTR induces aggresome formation and lung inflammation in cystic fibrosis through ROS-mediated autophagy inhibition. Nature Publishing Group 12, 863-875 (2010).

Ma, Y., Erkner, A., Gong, R., Yao, S., Taipale, J., Basler, K. & Beachy, P. Hedgehog-mediated patterning of the mammalian embryo requires transporter-like function of dispatched. Cell 111, 63-75 (2002).

Martín, V., Carrillo, G., Torroja, C. & Guerrero, I. The sterol-sensing domain of Patched protein seems to control Smoothened activity through Patched vesicular trafficking. Curr Biol 11, 601-607 (2001).

Martinelli, D.C. & Fan, C. Gas1 extends the range of Hedgehog action by facilitating its signaling. Genes Dev 21, 1231-1243 (2007).

Matise, M.P. & Wang, H. Sonic Hedgehog Signaling in the™Developing CNS. Growth Factors in Development 97, 75-117 (Elsevier Inc.: 2011).

Misra, S., Beach, B.M. & Hurley, J.H. Structure of the VHS Domain of Human Tom1 (Target of Myb 1): Insights into Interactions with Proteins and Membranes ‡. Biochemistry 39, 11282-11290 (2000).

Nakamura, M., Tanaka, H., Nagayoshi, Y., Nakashima, H., Tsutsumi, K., Ohtsuka, T., Takahata, S., Tanaka, M. & Okada, H. Targeting the hedgehog signaling pathway with interacting peptides to Patched-1. J. Gastroenterol. 47, 452-460 (2012).

Nowak, M., Machate, A., Yu, S.R., Gupta, M. & Brand, M. Interpretation of the FGF8 morphogen gradient is regulated by endocytic trafficking. Nature Publishing Group 13, 153-158 (2011).

Oglesby, I.K., Bray, I., Chotirmall, S., Stallings, R., O'Neill, S., McElvaney, N., & Greene, C. miR-126 is downregulated in cystic fibrosis airway epithelial cells and regulates TOM1 expression. J. Immunol. 184, 1702-1709 (2010).

Olzmann, J. & Chin, L. Aggresome Formation and Neurodegenerative Diseases: Therapeutic Implications. Curr Med Chem 15, (2008).

Penhieter, S., Mitchell, H., Garamszegi, N., Edens, M., Doré, J. & Leof, E. Internalization-Dependent and-Independent Requirements for Transforming Growth Factor ß Receptor Signaling via the Smad Pathway. Mol Cell Biol 22. 4750-4759 (2002).

Petralia, R.S., Schwartz, C.M., Wang, Y., Mattson, M.P. & Yao, P.J. Subcellular localization of patched and smoothened, the receptors for sonic hedgehog signaling, in the hippocampal neuron. J. Comp. Neurol. 519, 3684-3699 (2011).

Petralia, R.S., Wang, Y., Mattson, M.P. & Yao, P.J. Subcellular Distribution of Patched and Smoothened in the Cerebellar Neurons. Cerebellum (2012).doi:10.1007/s12311-012-0374-6

Piper, R.C. & Lehner, P.J. Endosomal transport via ubiquitination. Trends in Cell Biology 21, 647-655 (2011).

Platta, H.W. & Stenmark, H. Endocytosis and signaling. Current Opinion in Cell Biology 23, 393-403 (2011).

Porter, J., Ekker, S., Park, W., Kessler, D., Young, K., Chen, C., Ma, Y., Woods, A., Cotter, R., Koonin, E. & Beachy, P. Hedgehog patterning activity: role of a lipophilic modification mediated by the carboxy-terminal autoprocessing domain. Cell 86, 21-34 (1996).

Raiborg, C. & Stenmark, H. Hrs and endocytic sorting of ubiquitinated membrane proteins. Cell Struct. Funct. 27, 403-408 (2002).

Raiborg, C. & Stenmark, H. The ESCRT machinery in endosomal sorting of ubiquitylated membrane proteins. Nature 458, 445-452 (2009).

Ribes, V. & Briscoe, J. Establishing and Interpreting Graded Sonic Hedgehog Signaling during Vertebrate Neural Tube Patterning: The Role of Negative Feedback. Cold Spring Harbor Perspectives in Biology 1, a002014-a002014 (2009).

Rink, J., Ghigo, E., Kalaidzidis, Y. & Zerial, M. Rab conversion as a mechanism of progression from early to late endosomes. Cell 122, 735-749 (2005).

Rohatgi, R., Milenkovic, L. & Scott, M.P. Patched1 Regulates Hedgehog Signaling at the Primary Cilium. Science 317, 372-376 (2007).

Rowitch, D., St.-Jacques, B., Lee, S., Flax, J., Snyder, E. & McMahon, A. Sonic hedgehog regulates proliferation and inhibits differentiation of CNS precursor cells.

Rubinsztein, D.C., Codogno, P. & Levine, B. Autophagy modulation as a potential therapeutic target for diverse diseases. Nat Rev Drug Discov 11, 709-730 (2012).

Rusten A., Filimoneko, M., Rodahl, L., Stenmark, & Simonsen, A. ESCRTing autophagic clearance of aggregating Proteins. Autophagy, 2, 233-236 (2008).

Rusten, T.E. & Stenmark, H. How do ESCRT proteins control autophagy? Journal of Cell Science 122, 2179-2183 (2009).

Schwarz, L.A. & Patrick, G.N. Ubiquitin-dependent endocytosis, trafficking and turnover of neuronal membrane proteins. Molecular and Cellular Neuroscience 49, 387-393 (2012).

Scott, C. & Ioannou, Y.A. The NPC1 protein: structure implies function. Biochimica et Biophysica Acta (BBA) - Molecular and Cell Biology of Lipids 1685, 8-13 (2004).

Seet, L., Liu, N., Hanson, B.J. & Hong, W. Endofin recruits TOM1 to endosomes. J. Biol. Chem. 279, 4670-4679 (2004).

Shiba, Y. GAT (GGA and Tom1) Domain Responsible for Ubiquitin Binding and Ubiquitination. Journal of Biological Chemistry 279, 7105-7111 (2003).

Sigismund, S., Confalonieri, S., Ciliberto, A., Polo, S., Scita, G., & Di Fiore, P. Endocytosis and Signaling: Cell Logistics Shape the Eukaryotic Cell Plan. Physiol. Rev. 92, 273-366 (2012).

Slade, I., Murray, A., Hanks, S., Kumar, A., Walker, L., Hargrave, D., Douglas, J., Stiller, C., Izatt, L., & Rahman. Heterogeneity of familial medulloblastoma and contribution of germline PTCH1 and SUFU mutations to sporadic medulloblastoma. Familial Cancer 10, 337-342 (2010).

Stamataki, D. A gradient of Gli activity mediates graded Sonic Hedgehog signaling in the neural tube. Genes Dev 19, 626-641 (2005).

Stanton, B.Z. & Peng, L.F. Small-molecule modulators of the Sonic Hedgehog signaling pathway. Mol. BioSyst. 6, 44 (2009).

Strutt, H., Thomas, C., Nakano, Y., Stark, D., Neave, B., Taylor, A., & Ingham.P. Mutations in the sterol-sensing domain of Patched suggest a role for vesicular trafficking in Smoothened regulation. Curr Biol 11, 608-613 (2001).

Tabata, T. & Kornberg, T.B. Hedgehog is a signaling protein with a key role in patterning Drosophila imaginal discs. Cell 76, 89-102 (1994).

Taipale, J., Cooper, M.K., Maiti, T. & Beachy, P.A. Patched acts catalytically to suppress the activity of Smoothened. Nature 418, 892-897 (2002).

Thibert C., Teillet, M., Lapointe, F., Mazelin, L, Douarin, N. & Mehlen. Inhibition of Neuropeithelial Patched Induced Apoptosis by Sonic Hedgehog. Science 301, 843-846 (2003).

Tian, H. Mouse Disp1 is required in sonic hedgehog-expressing cells for paracrine activity of the cholesterol-modified ligand. Development 132, 133-142 (2004).

Torroja, C., Gorfinkiel, N. & Guerrero, I. Patched controls the Hedgehog gradient by endocytosis in a dynamin-dependent manner, but this internalization does not play a major role in signal transduction. Development 131, 2395-2408 (2004).

Toy, W., Lim, S.K., Loh, M.C.S. & Lim, Y. EGF-induced tyrosine phosphorylation of Endofin is dependent on PI3K activity and proper localization to endosomes. Cell Signal 22, 437-446 (2010).

Tumbarello, D., Waxse, B., Arden, S., Bright, N., Kendrick-Jones, J. & Buss, F. Autophagy receptors link myosin VI to autophagosomes to mediate Tom1-dependent autophagosome maturation and fusion with the lysosome. Nature Publishing Group 14, 1024-1035 (2012).

Uhlen M, Oksvold P, Fagerberg L, Lundberg E, Jonasson K, Forsberg M,Zwahlen M, Kampf C, Wester K, Hober S, Wernerus H, Björling L, Ponten F. Towards a knowledge-based Human Protein Atlas. Nat Biotechnol 28, 1248-50 (2010)

Vaillant, C. & Monard, D. SHH Pathway and Cerebellar Development. Cerebellum 8, 291-301 (2009).

Wang, T., Liu, N.S., Seet, L. & Hong, W. The emerging role of VHS domain-containing Tom1, Tom1L1 and Tom1L2 in membrane trafficking. Traffic 11, 1119-1128 (2010).

Wang, Y., Pennock, S.D., Chen, X., Kazlauskas, A. & Wang, Z. Platelet-derived growth factor receptor-mediated signal transduction from endosomes. J. Biol. Chem. 279, 8038-8046 (2004).

Wang, Y., Zhou, Z., Walsh, C.T. & McMahon, A.P. Selective translocation of intracellular Smoothened to the primary cilium in response to Hedgehog pathway modulation. Proc Natl Acad Sci USA 106, 2623-2628 (2009).

Wiley, S., & Burke, P. Regulation of receptor tyrosine kinase signaling by endocytic trafficking. Traffic 2, 12-18 (2001)

Wilson, C., Nguyen, C., Chen, M., Yang, J., Gacayan, R., Huang, J., Chen, J. & Chuang, P. Fused has evolved divergent roles in vertebrate Hedgehog signalling and motile ciliogenesis. Nature 459, 98-102 (2009).

Wolpert, L. Positional information and the spatial pattern of cellular differentiation. J. Theor. Biol. 25, 1-47 (1969).

Yamakami, M., Yoshimori, T. & Yokosawa, H. Tom1, a VHS domain-containing protein, interacts with tollip, ubiquitin, and clathrin. J. Biol. Chem. 278, 52865-52872 (2003).

Yamakami, M. & Yokosawa, H. Tom1 (target of Myb 1) is a novel negative regulator of interleukin-1- and tumor necrosis factor-induced signaling pathways. Biol. Pharm. Bull. 27, 564-566 (2004).

Zhu, A.J., Zheng, L., Suyama, K. & Scott, M.P. Altered localization of Drosophila Smoothened protein activates Hedgehog signal transduction. Genes Dev 17, 1240-1252 (2003).